A Section 508–conformant HTML version of this article is available at https://doi.org/10.1289/EHP2200.

# Mutagenicity and Lung Toxicity of Smoldering vs. Flaming Emissions from Various Biomass Fuels: Implications for Health Effects from Wildland Fires

*Yong Ho Kim,[1,2] Sarah H. Warren,[3] Q. Todd Krantz,[1] Charly King,[1] Richard Jaskot,[1] William T. Preston,[4] Barbara J. George,[5] Michael D. Hays,[6] Matthew S. Landis,[7] Mark Higuchi,[1] David M. DeMarini,[3] and M. Ian Gilmour[1]*

[1]Environmental Public Health Division, National Health and Environmental Effects Research Laboratory, U.S. Environmental Protection Agency, Research Triangle Park, North Carolina, USA
[2]National Research Council, Washington, DC, USA
[3]Integrated Systems Toxicology Division, National Health and Environmental Effects Research Laboratory, U.S. Environmental Protection Agency, Research Triangle Park, North Carolina, USA
[4]Consolidated Safety Services (CSS), Durham, North Carolina, USA
[5]Immediate Office, National Health and Environmental Effects Research Laboratory, U.S. Environmental Protection Agency, Research Triangle Park, North Carolina, USA
[6]Air Pollution Prevention and Control Division, National Risk Management Research Laboratory, U.S. Environmental Protection Agency, Research Triangle Park, North Carolina, USA
[7]Exposure Methods and Measurement Division, National Exposure Research Laboratory, U.S. Environmental Protection Agency, Research Triangle Park, North Carolina, USA

**Background:** The increasing size and frequency of wildland fires are leading to greater potential for cardiopulmonary disease and cancer in exposed populations; however, little is known about how the types of fuel and combustion phases affect these adverse outcomes.

**Objectives:** We evaluated the mutagenicity and lung toxicity of particulate matter (PM) from flaming vs. smoldering phases of five biomass fuels, and compared results by equal mass or emission factors (EFs) derived from amount of fuel consumed.

**Methods:** A quartz-tube furnace coupled to a multistage cryotrap was employed to collect smoke condensate from flaming and smoldering combustion of red oak, peat, pine needles, pine, and eucalyptus. Samples were analyzed chemically and assessed for acute lung toxicity in mice and mutagenicity in *Salmonella*.

**Results:** The average combustion efficiency was 73 and 98% for the smoldering and flaming phases, respectively. On an equal mass basis, PM from eucalyptus and peat burned under flaming conditions induced significant lung toxicity potencies (neutrophil/mass of PM) compared to smoldering PM, whereas high levels of mutagenicity potencies were observed for flaming pine and peat PM compared to smoldering PM. When effects were adjusted for EF, the smoldering eucalyptus PM had the highest lung toxicity EF (neutrophil/mass of fuel burned), whereas smoldering pine and pine needles had the highest mutagenicity EF. These latter values were approximately 5, 10, and 30 times greater than those reported for open burning of agricultural plastic, woodburning cookstoves, and some municipal waste combustors, respectively.

**Conclusions:** PM from different fuels and combustion phases have appreciable differences in lung toxic and mutagenic potency, and on a mass basis, flaming samples are more active, whereas smoldering samples have greater effect when EFs are taken into account. Knowledge of the differential toxicity of biomass emissions will contribute to more accurate hazard assessment of biomass smoke exposures. https://doi.org/10.1289/EHP2200

## Introduction

Each year, tens of millions of people globally experience destructive wildland fires and subsequent health impacts from smoke exposure (Levine et al. 1999). Trends for warmer and drier conditions are expected to result in greater frequency, size, and intensity of wildfires in many parts of the world (Abatzoglou and Williams 2016; Landis et al. 2017; Westerling et al. 2006). Besides the damage caused by fire itself, smoke emitted from fires is a serious public health concern. Biomass smoke is associated with increased incidence and severity of cardiopulmonary disease, and is recognized by the World Health Organization as a probable human lung carcinogen (IARC 2010; Straif et al. 2006). Consequently, the health risks due to short- and long-term exposure to wildland fire (or biomass burning) smoke are important for firefighters as well as for people living in communities near or downwind of wildland fires (Adetona et al. 2016).

Recent reviews cite numerous studies that have reported associations between wildland fires and health outcomes, including respiratory infections, asthma, cardiovascular diseases, and mortality (Liu et al. 2015; Reid et al. 2016). More specifically, it was estimated in one report that worldwide exposures to fine-fraction (<2.5 μm) particulate matter ($PM_{2.5}$) from wildland fires during 1997–2006 were associated with approximately 340,000 deaths per year, with larger numbers of deaths during years with dryer conditions and more fires (Johnston et al. 2012). In the United States, increases in forest fires during recent decades have been attributed in part to changing weather patterns that may continue to increase the likelihood, scale, and severity of fires in the future (Abatzoglou and Williams 2016; Westerling et al. 2006).

Despite the public health threat from an increased exposure to wildland fire smoke, studies examining the specific role of smoke components on disease incidence or severity following exposure are lacking. Specifically, it is important to determine whether the chemical composition of the emissions vary with the types of fuel burned and combustion conditions (flaming vs. smoldering), and how these variables affect the potential health effects of the resulting emissions. Of the myriad components in wildland fire smoke, primary and secondarily formed PM are major factors of concern because they can remain in the air for days or weeks and can be transported over long distances (Reisen et al. 2015). The spatiotemporal variability of PM, including smoldering vs. flaming emissions, can

Address correspondence to: M.I. Gilmour, Environmental Public Health Division, National Health and Environmental Effects Research Laboratory, U.S. Environmental Protection Agency, 109 T.W. Alexander Drive, Research Triangle Park, North Carolina 27709 USA. Telephone: (919) 541-0015. Email: gilmour.ian@epa.gov

Supplemental Material is available online (https://doi.org/10.1289/EHP2200).

The authors declare they have no actual or potential competing financial interests.

Received 12 May 2017; Revised 15 December 2017; Accepted 15 December 2017; Published 26 January 2018.

complicate the characterization of health risks of wildland fire smoke exposure to firefighters and the general public (Adetona et al. 2016).

Several studies have compared the chemical composition of PM from wildland fires or laboratory combustions of different fuel types under different burning conditions (Burling et al. 2010; Gilman et al. 2015; McMeeking et al. 2009; Reid et al. 2005); however, less work has integrated these findings with toxicological effects of the emissions. Moreover, due to considerable variability in study design and combustion conditions within and among laboratories, it is difficult to compare the toxicological findings across reported studies.

To address these issues, we generated biomass smoke during flaming or smoldering phases of combustion from five different fuel types using a quartz-tube furnace coupled to a multistage cryotrap system. We burned red oak, peat, pine needles, pine, and eucalyptus under flaming and smoldering phases to represent contrasting fuel types. These fuel types were selected as surrogates for major forest types across the United States. We assessed the resulting PM for lung toxicity in mice by measuring a panel of biomarkers after oropharyngeal aspiration and for mutagenicity in the *Salmonella* mutagenicity assay.

The data are presented in two ways: *a*) as a potency expressed as toxicity per mass of PM, which can be used to facilitate understanding and qualitative prediction of potential health effects, and *b*) as an emission factor (EF), which reflects exposure based on mass of fuel consumed, and can be further expressed by thermal energy of fuel combustion. These latter analyses were performed in order to provide information on how wildfire emissions and potential health effects can be quantified based on fuel consumption and to provide comparison with emissions from other fuels and combustion processes.

## Methods

### *Fuel Types*

We burned five different biomass fuels in this study: northern red oak (*Quercus rubra*), pocosin peat, ponderosa pine (*Pinus ponderosa*) needles, lodgepole pine (*Pinus contorta*), and eucalyptus (*Eucalyptus globulus*). Red oak was used to represent eastern and central wildland fires in the United States and was obtained from the Air and Energy Management Division at the U.S. Environmental Protection Agency (EPA). Peat was used to represent peatland/coastal wildfires, which are found mostly in the midwestern and southeastern United States, and was collected from the coastal oligotrophic plain of eastern North Carolina (Alligator River National Wildlife Refuge) using a Russian peat borer tool (De Vleeschouwer et al. 2010). Ponderosa pine needles and lodgepole pine were used to represent western wildland fires in the United States and were provided by the U.S. Forest Service Missoula Fire Sciences Laboratory. Eucalyptus (purchased commercially from Woodworkers Source) was used to represent chaparral (i.e., fire-prone) biome-type wildland fires, which are found in most of the southern part of coastal California in the United States as well as other continents (e.g., the west coast of South America and southwestern Australia) (Kellison et al. 2013). The red oak, pine, and eucalyptus samples were cut into approximately 2-cm-long wood chips to facilitate uniform combustion conditions. The peat sample was crumbled into a loose agglomerate, whereas the pine needles were burned without further processing. All biomass fuels were stored in a temperature- and humidity-controlled room (23°C and 39% relative humidity) until used.

### *Combustion and Smoke Collection*

Biomass combustion was conducted in a quartz-tube furnace (Klimisch et al. 1980; Werley et al. 2009) under both smoldering and flaming phases (Figure 1). This system consisted of a quartz tube (1 m long and 3.8 cm diameter) and a ring furnace (11.4 cm long). The furnace surrounding the quartz tube was mounted on a linear actuator driven with a combination travel speed controller that was set to maintain a speed of 1 cm/min as it traversed along the length of the quartz tube. The biomass fuel (15 g) was placed uniformly inside the length of the quartz tube, and the temperature was adjusted to achieve steady-state smoldering (approximately 500°C) and flaming (approximately 640°C) combustion conditions (Figure S1). The furnace system was able to sustain stable flaming or smoldering phases consistently for 60 min. The primary air flow (air through the quartz tube) was approximately 2 L/min.

We collected the smoke using a multistage cryotrap system (Figure 1). This system was employed for two principal reasons: *a*) to collect volatile and semivolatile components, which typically pass through filters, and *b*) to collect particles, which are difficult to extract from filter matrixes. Half of the outlet biomass smoke flow (approximately 1 L/min) from the tube furnace was drawn into the cryotrap system consisting of three sequential impingers maintained at −10°C, −50°C, and −70°C. PM and condensable gas-phase semivolatiles in the biomass smoke (termed smoke condensate henceforth) were captured by cryogenic trapping in the impingers. Each impinger was packed with mixed-size glass beads (1 and 0.4 cm diameter) to provide a large surface area for collection of the smoke. The other half of the biomass smoke flow (approximately 1 L/min) was diluted with secondary air flow (15 L/min) and then analyzed continuously for carbon dioxide ($CO_2$) and carbon monoxide (CO) using a nondispersive infrared analyzer (602 $CO/CO_2$; CAI, Inc.).

We also collected PM on glass–fiber filters installed in both the exhaust line of the tube furnace and the cryotrap system exhaust during the combustion (60 min) and determined mean PM concentrations gravimetrically by weighing the filter before and after PM collection. Particle-size distributions (in the range of 32 nm to 10.57 μm) were monitored in real time by an electrical low-pressure impactor (ELPI; model 97-2E; Dekati Ltd.). Number-based size distribution data were converted into the surface area–weighted distributions using the ELPIvi software (version 3.0; Dekati Ltd.) (Schmid and Stoeger 2016). Flow rates of the biomass smoke were precisely controlled by a vacuum controller (XC-40; Apex Instruments, Inc.) located at the end of each exhaust line. A pressure gauge (Magnehelic®, Dwyer Instruments Inc.) was placed in the outlet of the tube furnace to ensure a constant pressure drop throughout each burn.

### *Characterization of Biomass Smoke*

Concentrations of $CO_2$, CO, and PM were used to routinely characterize the biomass smoke emissions. Flaming and smoldering combustion phases are typically characterized by modified combustion efficiency (MCE), which is defined as $\mathrm{MCE}\,(\%) = [\Delta CO_2/(\Delta CO_2 + \Delta CO)] \times 100$, where $\Delta CO_2$ and $\Delta CO$ are the excess concentrations of $CO_2$ and CO (Ward and Radke 1993). We considered combustion to be flaming when the MCE was >95% and smoldering when MCE was 65–85%, as suggested by Urbanski (2014).

Smoke properties are also described using EFs, which are defined as the mass of species $t$ emitted per mass of dry fuel consumed, which can be calculated as $\mathrm{EF}\,t(\mathrm{g/kg}) = (\mathrm{F}c \times \mathrm{C}t \times \mathrm{M}t \times 1{,}000)/(\mathrm{M}c \times \mathrm{C}_T)$, where F$c$ is the mass fraction of carbon in the dry biomass fuel (assumed to be 0.5), M$t$ is the molar mass of species $t$, M$c$ is the molar mass of carbon, $\mathrm{C}_T$ is the total mass of carbon associated to all species in the biomass smoke, and C$t$ is the mass of carbon emitted as species $t$, and given by $Ct(\mathrm{mg/m^3}) = (\mathrm{M}c \times N \times \mathrm{V}t)/24.45$, where $N$ is the number of carbon atoms in species $t$, and V$t$ is the concentration of species $t$ in ppm (Soares Neto et al. 2009). In order to validate EFs

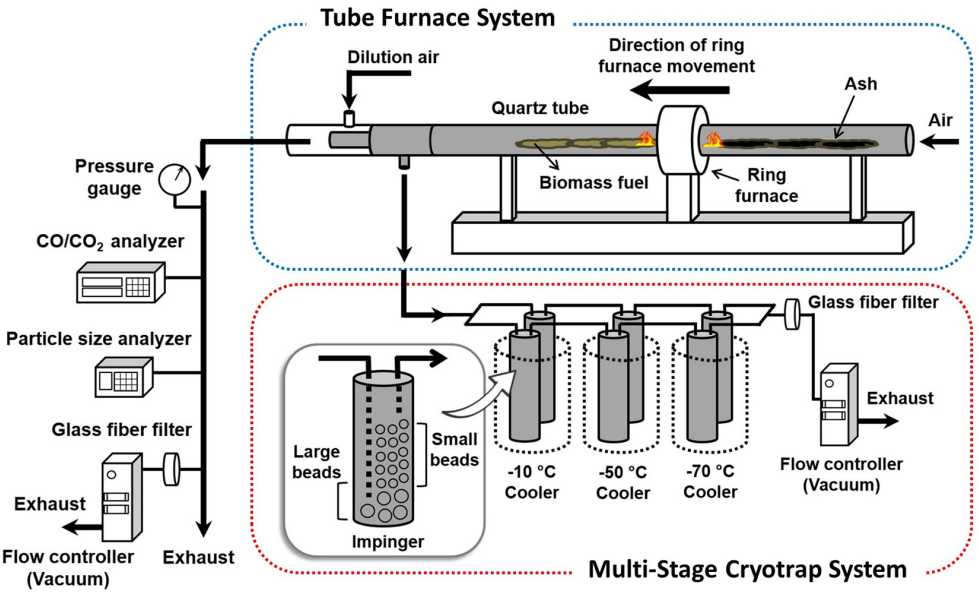


**Figure 1.** Diagram of the biomass combustion and smoke collection system. The tube furnace system consisted of a quartz tube and a ring furnace that traversed along the length of the quartz tube and was able to sustain stable flaming or smoldering phases consistently for 60 min. The multistage cryotrap system had three sequential impingers that were cooled cryogenically at −10, −50, and −70°C, permitting the capture of PM and semivolatile organic compounds from the biomass smoke emissions.

estimated from the tube furnace in the present study, EFs for CO, $CO_2$, and PM were compared with the published EFs from various fuel combustion conditions (in-ground vs. aboveground biomass fuels). We also expressed EFs per megajoule$_{thermal}$ ($MJ_{th}$) by using the heat energy ($MJ_{th}$/kg) of each fuel burned, which was 21.70 for the red oak (Ince 1979), 23.00 for the peat (Morvay and Gvozdenac 2008), 11.96 for the pine needles (de Muñiz et al. 2014), 20.00 for the pine (Nielson et al. 1985), and 19.25 for the eucalyptus (de Muñiz et al. 2014).

### *Biomass Smoke Condensate Analysis*

Following the combustion tests, we extracted smoke condensate from the cryogenically cooled impingers and loose beads by washing them with acetone. We then pooled the smoke condensate suspension and concentrated it with a rotary evaporator (Rotavapor® R-200; Buchi). The smoke condensate was then dried under nitrogen gas to obtain predominantly solid PM (termed dried smoke condensate or PM henceforth), which underwent subsequent analyses.

For carbon species analysis, the aliquot of the smoke condensate suspension was pipetted onto prebaked 1.5-cm$^2$ quartz filter punches, dried, and analyzed for organic carbon (OC) and elemental carbon with a carbon analyzer (107A; Sunset Laboratory, Inc.). The OC fraction was further analyzed for polar (methoxyphenols and levoglucosan) and nonpolar [polycyclic aromatic hydrocarbons (PAHs) and *n*-alkanes] organic compounds with a thermal desorption unit (TD; TDSA2/TDS, Gerstel, Inc.) coupled to a gas chromatograph-mass spectrometer (GC-MS; 6890/5973, Agilent Technologies, Inc.). A full list of the organic compounds is shown in Table S1. The TD-GC-MS sample load (0.5–1 μg OC/μL) was optimized or determined by the OC content measured by the thermo-optical method (Hays et al. 2002). A prebaked quartz filter punch was placed inside a glass TD tube and spiked with a deuterated internal standard solution (1 μL) and aliquot of the PM suspension (1 − 12 μL). Nitrogen (50 mL/min for 40 s) was used to evaporate solvent prior to TD-GC-MS analysis. An autosampler (TDSA2, Gerstel Inc.) was utilized to insert the glass tube into the TD unit, which heated the sample (325°C) under He (50 mL/min). Sample flow was directed to a cryogenically cooled inlet (−100°C), which was rapidly heated to 300°C following the desorption step. Semivolatile organic compounds (SVOC) were chromatographed using a capillary column (30 m long and 0.25 mm inside diameter; DB-5) ramped from 65 to 300°C. The MS was operated in single ion monitoring mode. A separate TD-GC-MS analysis for levoglucosan was performed by spiking 10 μL of the smoke condensate suspension with $^{13}$C levoglucosan internal standard (20 ng/μL) and reacting with 50 μL of N,O-bis(trimethylsilyl)trifluoroacetamide reagent for 30 min at 70°C. This mixture (1 μL) was spiked onto a Carbotrap F/Carbotrap C tube (Sigma-Aldrich) and dry purged under nitrogen and analyzed as described above. Samples were quantified using the internal standard method and expressed in μg/g units. SVOC concentrations were blank subtracted using an acetone solvent check (4 μL). A four-level calibration was established prior to sample analysis. The calibration ranged from 0.1 to 1 ng/μL for most PAH targets (total 28 PAHs including 16 EPA-regulated priority PAHs) and 0.63 to 6.25 ng/μL for most alkanes (total 36 alkanes). A midlevel check standard was run with each daily target set and used to assess the daily target recovery. If the midlevel check standard failed to pass the minimum agreement criterion for the number of acceptable targets, it was used as a daily continuing calibration, in which case an average response factor curve fit was used for quantification. Detection limits were established for each target listing. Raw values that fell below the detection limit threshold were listed as not detected.

For inorganic elemental analysis, the dried smoke condensate was digested in 3:1 aqua regia mixture (1 mL concentrated hydrochloric acid: 0.33 mL concentrated nitric acid, both Optima grade; Fisher Scientific) to leach trace elements. After dilution to a final concentration of 2% total acid, supernatants were separated by centrifugation (405 × g for 15 min at 22°C), then assayed for 44 target elements (listed in Table S2) by high-resolution-magnetic

sector field inductively coupled plasma mass spectrometry (HR-ICP-MS; ELEMENT™ 2; Thermo Scientific). In preparation for major ion analysis, the dried smoke condensate was diluted in 10 mL of American Society for Testing and Materials Type I ultrapure water (18.2 MΩ · cm), sonicated, and analyzed for nitrate ($NO_3^-$), sulfate ($SO_4^{2-}$), chloride ($Cl^-$), sodium ($Na^+$), ammonium ($NH_4^+$), potassium ($K^+$), magnesium ($Mg^{2+}$), phosphate ($PO_4^{3-}$), and calcium ($Ca^{2+}$) using a dual ion chromatography system (ICS-2000, Dionex). The smoke condensate suspension (in acetone) was solvent-exchanged into saline at a final concentration of 2 mg PM/mL and then further analyzed for pH and endotoxin levels. The pH value was measured with a calibrated pH meter (440; Corning®). For the endotoxin measurement, the dried smoke condensate suspension (in saline) was vortexed and sonicated to ensure homogeneity, and then diluted in endotoxin-free water at a concentration of 1 mg/mL. Endotoxin measurements were performed using the Limulus amebocyte lysate assay (QCL-1000™; Lonza) as per the manufacturer's protocol. Aliquots of the dried smoke condensate suspensions (in saline) were stored at −80°C until toxicity testing.

### *Experimental Animals*

Adult pathogen-free female CD-1 mice (approximately 20-g body weight) were purchased from Charles River Breeding Laboratories and were housed in groups of five in polycarbonate cages with hardwood chip bedding at the U.S. EPA Animal Care Facility, which is accredited by the Association for Assessment and Accreditation of Laboratory Animal Care, and were maintained on a 12-h light-to-dark cycle at 22.3 ± 1.1°C temperature and 50 ± 10% humidity. Mice were given access to rodent chow and water *ad libitum* and were acclimated for at least 10 d before the study began. Mice were treated humanely and with regard for alleviation of suffering. The studies were conducted after approval by the U.S. EPA Institutional Animal Care and Use Committee. Mice were weighed and weight-randomized into 24 groups of six mice each for each exposure condition.

### *Mouse Exposure to the PM*

We solvent-exchanged the smoke condensate suspension in acetone into saline to a final PM concentration of 2 mg/mL, and then administered it into the lungs of CD-1 mice at 100 μg in 50 μL by oropharyngeal aspiration. We performed oropharyngeal aspiration on mice anesthetized in a small plexiglass box using vaporized anesthetic isoflurane, following a previously described technique (Kim et al. 2014b). Briefly, the tongue of the mouse was extended with forceps, and 100 μg of PM in 50 μL saline was pipetted into the oropharynx. Immediately, the nose of the mouse was then covered, causing the liquid to be aspirated into the lungs. The selection of PM dose (100 μg) was based on the following information. Although PM exposure near wildland fires averages several hundred $\mu g/m^3$ (Naeher et al. 2007), some studies have identified peak values ranging from 1.9 $mg/m^3$ [measured $PM_{10}$ levels at a site in India heavily affected by haze from nearby wildland fires (Naeher et al. 2007)] to 2.8 $mg/m^3$ [respirable $PM_{3.5}$ levels experienced by firefighters while fighting a fire (Swiston et al. 2008)]. Note that the PM dose in this study was determined based on these extreme exposure values (Naeher et al. 2007; Swiston et al. 2008). Therefore, wildfire PM deposited in the human lungs for 24 h in this particular case [assuming a human respiratory minute volume and surface area of 20 L/min (NRC 1992) and 70 $m^2$ (Fröhlich et al. 2016), respectively] would be 78.2–115.2 $ng/cm^2$. Assuming a mouse respiratory minute volume and surface area of 0.0269 L/min (Bide et al. 2000) and 642 $cm^2$ (Weibel 1973), respectively, mice could inhale between 74 and 108 μg (equivalent to 114.5–168.8 $ng/cm^2$) of wildfire PM over a 24-h period. We chose a single PM dose of 100 μg because *a*) this dose represents a peak 24-h exposure for a wildfire event, and *b*) this dose (equivalent to 154 $ng/cm^2$ in mouse lungs) appeared to be relevant to the inhaled wildfire PM concentrations in the human lungs. Moreover, because the same PM dose was used in other lung toxicity studies (Gilmour et al. 2007; Kim et al. 2014a, 2014b, 2015), the chosen PM dose enabled us to examine the comparative lung toxicity of various inhaled particles. We instilled additional mice with 2 μg of lipopolysaccharide in 50 μL saline (LPS; *Escherichia coli* endotoxin; 011:B4 containing $10^6$ unit/mg material; Sigma-Aldrich) as a positive control to demonstrate maximal responsiveness to this well-characterized inflammatory agent. We also instilled additional mice with 50 μL saline alone as a negative control.

### *Lung Toxicity Assay*

At 4 and 24 h postexposure, six mice from each treatment group were euthanized with 0.1 mL intraperitoneal injection of Euthasol (diluted 1:10 in saline; 390 mg pentobarbital sodium and 50 mg phenytoin/mL; Virbac AH Inc.), and blood was collected by cardiac puncture using a 1-mL syringe containing 17 μL sodium citrate to prevent coagulation. The trachea was then exposed, cannulated, and secured with suture thread. The thorax was opened, and the left mainstem bronchus was isolated and clamped with a microhemostat. The right lung lobes were lavaged three times with a single volume of warmed Hanks balanced salt solution (HBSS; 35 mL/kg mouse). The recovered bronchoalveolar lavage fluid (BALF) was centrifuged at 300 × g for 10 min at 4°C, and the supernatant was stored at both 4°C (for biochemical analysis) and −80°C (for cytokine analysis). The pelleted cells were resuspended in 1 mL HBSS (Sigma-Aldrich). Total BALF cell count of each mouse was obtained by a Coulter counter (Beckman Coulter Inc.). Additionally, 200 μL resuspended cells were centrifuged in duplicate onto slides using a Cytospin™ (Shandon™) and subsequently stained with Diff-Quik solution (American Scientific Products) for enumeration of macrophages and neutrophils with at least 200 cells counted from each slide. Hematology values including total white blood cells, total red blood cells, hemoglobin, hematocrit, mean corpuscular volume, mean corpuscular hemoglobin concentration, and platelets were measured using a Coulter® AcT 10 Hematology Analyzer (Beckman Coulter, Inc.).

Albumin and total protein concentrations in BALF were measured by the SPQ™ test system (DiaSorin) and the Coomassie Plus Protein Assay (Pierce Chemical) with a standard curve prepared with bovine serum albumin (Sigma-Aldrich), respectively. Concentrations of lactate dehydrogenase (LDH) and γ-glutamyl transferase (GGT) in BALF were determined using commercially available kits (LDH-L Reagent and Gamma GT Reagent, Thermo Scientific). Activity of *N*-acetyl-β-D-glucoaminidase (NAG) in BALF was determined using a NAG assay kit (Roche Applied Science). All biochemical assays were modified for use on the KONELAB 30 clinical chemistry spectrophotometer analyzer (Thermo Clinical Lab Systems), as described previously (Kim et al. 2014a). Concentrations of tumor necrosis factor-α (TNF-α), interleukin-6 (IL-6) and macrophage inhibitory protein-2 (MIP-2) in BALF were determined using commercial multiplexed fluorescent bead-based immunoassays (MILLIPLEX® Map Kit, Milliore Co.) measured by a Luminex® 100™ (Luminex Co.) following the manufacturer's protocol. The limits of detection (LOD) of each cytokine were 6.27, 3.28, and 29.14 pg/mL for TNF-α, IL-6, and MIP-2, respectively, and all values below these lowest values were replaced with a fixed value of one-half of the LOD value.

We calculated the lung toxicity potency by determining the neutrophil counts in BALF (i.e., an equal PM mass basis). We

then multiplied these values (neutrophils/μg PM) by the calculated EF for PM (g PM/kg fuel) for each fuel and burning condition to give the lung toxicity EF (neutrophils/kg fuel).

### *Mutagenicity Assay*

For mutagenicity analysis, we dried the smoke condensate suspension under nitrogen gas (TurboVap II; Zymark), resuspended the dried smoke condensate in dichloromethane (DCM), sonicated it for 45 min, and filtered the extractable organic material (EOM) sequentially through 0.2- and 0.02-μm Anotop filters (Whatman, Midland Scientific Inc.). We determined the percentage EOM by gravimetric measurement performed by adding 100 μL of DCM extract to each of three preweighed aluminum weighing boats. The DCM was evaporated by heating the boats at 100°C until dry; then the cooled boats were weighed again. The three different weights were averaged and represented to micrograms of EOM/μL of DCM extract. We solvent-exchanged the EOM into dimethyl sulfoxide (DMSO) at 10 mg EOM/mL DMSO.

We performed the *Salmonella* plate-incorporation mutagenicity assay (Maron and Ames 1983) using the base-substitution strain TA100 [*hisG46 chl-1005 (bio uvrB gal) rfa-1001* pKM101$^+$ Fels-1$^+$ Fels-2$^+$ Gifsy-1$^+$ Gifsy-2$^+$] and the frameshift strain TA98 [*hisD3052 chl-1008 (bio uvrB gal) rfa-1001* pKM101$^+$ Fels-1$^+$ Fels-2$^+$ Gifsy-1$^+$ Gifsy-2$^+$] (Porwollik et al. 2001). We evaluated the EOM in the presence and absence of metabolic activation using S9 mix/plate composed of 1 mg S9 protein/500 μL of S9 mix (Maron and Ames 1983); S9 was an aroclor-induced Sprague-Dawley rat liver homogenate (Moltox). TA100 and TA98 have been used extensively to evaluate the mutagenicity of biomass emissions (Bell and Kamens 1990; IARC 2010). Strain TA100 + S9 detects base-substitution mutagens, such as PAHs, TA98 + S9 detects frameshift mutagens such as PAHs and aromatic amines, and TA98 − S9 detects nitroarenes. As positive controls, 2-aminoanthracene (for TA98 + S9 and TA100 + S9), 2-nitrofluorene (for TA98 − S9), and sodium azide (for TA100 − S9) were used, and DMSO was used as a negative control.

With some exceptions due to limited sample quantity, the samples were evaluated among nine doses (5, 10, 20, 25, 40, 100, 200, 250, and 500 μg EOM/plate) at one plate/dose in four independent experiments. We defined a positive mutagenic response as a reproducible, dose-related response with an increase in revertants (rev) per plate relative to the DMSO control from the four independent experiments. We calculated the mutagenic potency by determining the linear regressions over the linear portion of the dose–response curves created by the average of the primary data (rev/plate) from the four independent experiments (Figures S2 and S3). The linear portion was defined by the line with the highest coefficient of determination ($r^2$) value. Dose–response data outside of the linear portion were not used in the linear regressions because these resulted in a downturn in the curve and a reduction of the $r^2$ values.

We multiplied the mutagenic potencies of the EOM (rev/μg EOM) by the percentage EOM to give the mutagenic potencies of the PM (rev/μg PM) for each fuel/combustion condition. We then multiplied these values (rev/μg PM) by the calculated EF for PM (g PM/kg fuel) for each fuel and burning condition to give the mutagenicity EF (rev/kg fuel). We then converted the rev/kg fuel to rev/$MJ_{th}$ using the values for the heat energy of the fuels ($MJ_{th}$/kg) described in the "Characterization of Biomass Smoke" section. In order to evaluate the mutagenicity EFs of the biomass smoke in the present study, the rev/$MJ_{th}$ values were compared with the published mutagenicity EFs for red oak burned in cookstoves as well as for a variety of other emissions available from the literature.

### *Statistical Analysis*

For the analysis of lung toxicity data (pro-inflammatory cytokine, protein, albumin, NAG, LDH, and GGT values in BALF and hematology values), we used one-way analysis of variance (ANOVA) followed by the Dunnett's multiple comparison adjustment to compare the biological responses between PM-exposed groups and a negative control group. This analysis was performed using GraphPad Prism software (version 6.07; GraphPad Software, Inc.). We modeled neutrophil and *Salmonella* responses as dependent variables to characterize their association with different fuel types and combustion phases. This analysis was performed using SAS software for Windows (version 9.4; SAS Institute Inc.). For analysis of the neutrophil count data (lung toxicity), we used negative binomial regression in the SAS GENMOD procedure; for analysis of the *Salmonella* (mutagenicity) responses, we used two-way factorial ANOVA for fixed effects in the SAS MIXED procedure. Negative binomial regression is commonly used for overdispersed count data, that is, where the variance exceeds the mean, as observed for the neutrophil count data in this study (Diggle et al. 2002; Lawless 1987). The linear or log scale for statistical tests of the *Salmonella* responses was determined by evaluating normality of model residuals (Shapiro-Wilk test in SAS UNIVARIATE). We also modeled the lung toxicity EFs and mutagenicity EFs with linear regression analysis to characterize their association with the smoke emission characteristics (i.e., EFs for PAH, OC, and PM). This analysis was performed using GraphPad Prism software (version 6.07; GraphPad Software, Inc.). We expressed the data as mean ± standard error of the mean (SEM) and assigned the statistical significance level at a probability value of $p < 0.05$.

## Results

### *Properties of Smoldering and Flaming Combustion Emissions*

Specific properties, including MCE, PM size distribution, PM concentration, and pollutant EFs, of the smoke from five biomass fuels (red oak, peat, pine needles, pine, and eucalyptus) and two combustion phases (smoldering and flaming) are listed in Table 1. The MCE values were 63–83% during the smoldering and 97–99% during the flaming phase. For all fuel types, the median diameters for the PM based on surface area–weighted particle size distributions from the smoldering phase were >1 μm (mean = 2.04 μm), whereas those from the flaming phase were <1 μm (mean = 0.59 μm).

The mean ± SEM of the EFs for CO, $CO_2$, and PM of the smoldering phase smoke was 233 ± 26, 1,026 ± 74, and 121 ± 16 g/kg fuel, respectively, whereas the average EFs for CO and PM of the flaming phase smoke were decreased to 22 ± 3 and 1 ± 0 g/kg fuel, respectively. In contrast, the average EF for $CO_2$ increased with flaming combustion to 1,795 ± 5 g/kg fuel. These data confirm that the flaming combustion conditions were more efficient, converting much of the carbon to $CO_2$, whereas more carbonaceous PM and CO were emitted during smoldering.

We plotted the pollutant EFs for CO, $CO_2$, and PM as a function of the MCE, and compared their relationships with published field and laboratory measurement data (Figure 2). Except for the EFs developed for smoldering peat, EFs were linearly dependent on the MCE of each fuel, and the linear trends were fitted to the published data obtained from aboveground fuel combustions ($r^2 = 0.97$, $r^2 = 0.82$, and $r^2 = 0.86$ of EFs for CO, $CO_2$, and PM, respectively) (McMeeking et al. 2009). Although the EFs of the peat smoke fell outside the linear trend lines and this deviation increased in the plot of the EF for PM vs. the MCE, they were in good

**Table 1.** Characteristics and emission factors (EFs) of the biomass smoke emitted from the tube furnace system.

| | Red oak | | Peat | | Pine needles | | Pine | | Eucalyptus | |
|---|---|---|---|---|---|---|---|---|---|---|
| Variable | Smoldering | Flaming | Smoldering | Flaming | Smoldering | Flaming | Smoldering | Flaming | Smoldering | Flaming |
| Characteristic (unit) | | | | | | | | | | |
| MCE (%)[a] | 73 ± 1 | 99 ± 0 | 71 ± 1 | 97 ± 0 | 83 ± 0 | 98 ± 0 | 76 ± 1 | 98 ± 0 | 63 ± 1 | 98 ± 0 |
| PM size (μm)[b] | 1.38 (1.22) | 0.65 (2.09) | 2.73 (1.41) | 0.89 (2.96) | 2.70 (1.40) | 0.54 (1.27) | 2.37 (2.76) | 0.40 (1.46) | 1.02 (2.90) | 0.48 (1.41) |
| CO (ppm) | 793 ± 30 | 80 ± 6 | 1,385 ± 135 | 159 ± 10 | 602 ± 34 | 121 ± 8 | 766 ± 25 | 105 ± 14 | 1,201 ± 53 | 109 ± 10 |
| $CO_2$ (ppm) | 2,167 ± 111 | 5,597 ± 173 | 3,425 ± 373 | 5,042 ± 161 | 3,067 ± 192 | 6,576 ± 161 | 2,458 ± 120 | 6,844 ± 222 | 2,058 ± 67 | 6,407 ± 160 |
| PM ($mg/m^3$) | 973 | 8 | 488 | 15 | 624 | 18 | 1,050 | 14 | 1,418 | 10 |
| Emission factor (g/kg fuel)[c] | | | | | | | | | | |
| CO | 231 | 16 | 288 | 33 | 154 | 20 | 198 | 21 | 292 | 20 |
| $CO_2$ | 990 | 1,804 | 1,120 | 1,777 | 1,233 | 1,797 | 999 | 1,797 | 787 | 1,798 |
| PM | 131 | 1 | 71 | 1 | 98 | 1 | 143 | 1 | 160 | 1 |

Note: Error ranges represent standard error of the mean (SEM). PM, particulate matter.
[a]Modified combustion efficiency (MCE) = $\Delta CO_2/(\Delta CO_2 + \Delta CO)$.
[b]Surface median aerodynamic diameters calculated from surface area–weighted particles size distributions; values in brackets represent the geometric standard deviation (GSD) of the particle size distributions.
[c]Emission factor (EF)$t$(g/kg) = (fuel carbon fraction × mass of carbon emitted as $t$ × molecular weight $t$ × 1,000)/(molecular weight carbon × total mass of carbon).

agreement with the published EFs of smoldering phase smoke from ground fuel combustions (e.g., duff and organic soils) (Urbanski 2014) and peatland wildfires (Geron and Hays 2013) ($r^2 = 0.83$, $r^2 = 0.93$, and $r^2 = 0.61$ of EFs for CO, $CO_2$, and PM, respectively) (Figure 2).

The major chemical compounds measured in the biomass smoke condensate samples are shown in Figure 3 and Table 2; more details on ionic, inorganic, and semivolatile organic species are presented in Tables S3–S5. Depending on the sample, the smoldering combustion emitted 4–49 times more PM (or dried smoke condensate) mass than flaming combustion, but endotoxin (average of 329 and 241 endotoxin units (EU)/g for smoldering and flaming, respectively) and pH levels (average pH of 3.57 and 3.67 for smoldering and flaming, respectively) of the PM were similar on a mass basis between the two combustion conditions (Table 2). The wood smoke condensate samples (i.e., red oak, pine, and eucalyptus) averaged 56 and 60% (of PM mass) total carbon for smoldering and flaming, respectively, whereas the nonwood smoke condensate samples (i.e., peat and pine needles) had a slightly higher percentage of total carbon for smoldering (average of 76% of PM mass) but lower for flaming (average of 43% of PM mass) combustion.

Ionic species (mostly $Cl^-$, $SO_4^{2-}$, and $PO_4^{3-}$) accounted for <1% and 15.6% of PM in the smoke condensate samples from smoldering and flaming combustion, respectively (Figure 3 and Table S3). Similarly, inorganic species (mostly Ca, Na, S, and metals) of the smoke condensate collected from smoldering contributed to an average of 1% of PM mass, and inorganic species from flaming samples contributed to an average of 6% of PM mass (Figure 3 and Table S4). The peat flaming smoke condensate contained the highest level of heavy metals (e.g., Cr, Cu, Fe, Ni, Pb, Sb, and Zn), accounting for up to 1.2% of PM mass. For both the flaming and smoldering conditions, the wood smoke condensate was enriched in levoglucosan (up to 12.6% of PM mass) compared with the nonwood smoke condensate (up to 4.1% of PM mass), whereas total methoxyphenols made up a higher percentage of the PM mass in smoldering smoke condensate (up to 6.5% of PM mass) than in flaming smoke condensate (up to 1.6% of PM mass) for all fuel types (Figure 3 and Table S5). Levels of *n*-alkanes and PAHs in the smoke condensate samples also varied on the basis of combustion conditions and fuel type (Figure 3 and Table S5). *N*-alkanes contributed the most to PM mass (0.9%) in the smoke condensate sample from smoldering peat, whereas the highest contributions of PAHs (0.5%) were found in the smoke condensate samples following flaming combustion of the pine and eucalyptus, respectively. Overall, the toxic heavy metals and PAHs were relatively enriched in the flaming smoke condensate samples; more specifically, nonwood smoke condensate comprised up to 12,247 μg/g of heavy metals (Table S4) and wood smoke condensate contained up to 5,138 μg/g of PAHs (Table S5).

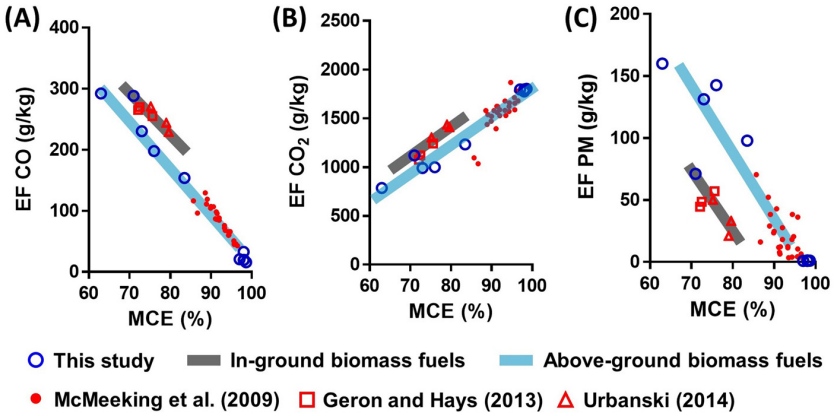


**Figure 2.** Comparison of emission factors (EFs) estimated from the tube furnace system in this study with published EFs from various fuel combustion. (*A*), (*B*), and (*C*) pollutant EFs for CO, $CO_2$, and PM vs. modified combustion efficiency (MCE). Open circles are pollutant EFs estimated in this study. Solid dots represent pollutant EFs from the open combustion of various plant fuels (McMeeking et al. 2009). Open squares are pollutant EFs from peatland wildfires (Geron and Hays 2013). Open triangles are pollutant EFs from the smoldering combustion of ground biomass fuels, such as duff and organic soils (Urbanski 2014). McMeeking et al. (2009) Geron and Hays (2013) Urbanski (2014).

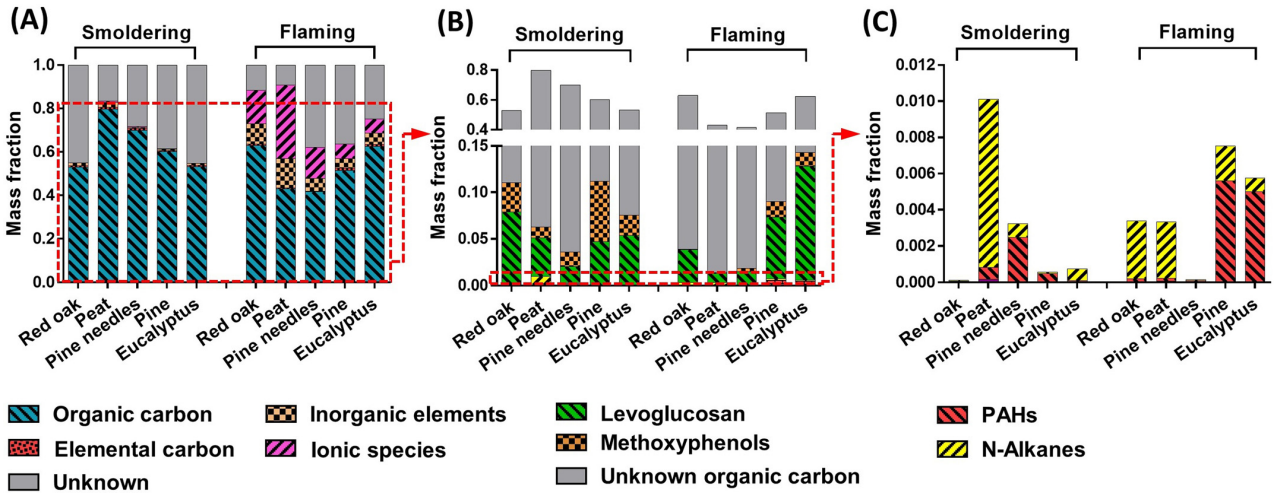


**Figure 3.** Chemical components in the biomass smoke condensate collected from different fuel types and combustion phases. (*A*) mass fraction of major chemical compounds, (*B*) organic carbon species [the dashed line, superimposed on (*A*)], and (*C*) semivolatile compounds [the dashed line, superimposed on (*B*)] in the biomass smoke condensate from smoldering and flaming combustion.

### *Lung Toxicity Potencies of the Biomass Smoke Particulate Matter*

After exposing mice to an equal mass (100 μg) of the PM samples, we analyzed the BALF for markers of lung toxicity, including markers of lung inflammation (neutrophils and macrophages), pro-inflammatory cytokines (IL-6, TNF-α, and MIP-2), and markers of cellular injury (protein, albumin, NAG, LDH, and GGT) (Figures 4 and 5 and Tables S6–S8). Neutrophil counts (per mass of PM) were highest in mice exposed to the flaming peat and eucalyptus PM at 4 h (Figure 4 and Table S6). The average proportion of neutrophils relative to the total number of BALF cells was 22% following both exposures, compared with only 2% in controls at 4 h. At 24 h, BALF neutrophil counts in the mice exposed to the flaming peat and eucalyptus PM were higher than (or similar to) counts in exposed mice evaluated at 4 h, and neutrophils accounted for 44 and 21% of total lavageable cells on average, respectively, compared with 2% in controls (Figure 4). The flaming peat and eucalyptus PM were associated with significantly higher neutrophil recruitment than other fuel PM samples at 24 h postexposure. The total numbers of macrophages were similar for each PM sample in mice evaluated 4 and 24 h postexposure (Figure 5A and Table S6).

Further analysis of pro-inflammatory cytokines in BALF revealed that the concentrations of IL-6, TNF-α, and MIP-2 were significantly elevated in mice exposed only to the flaming peat PM at 4 h, compared with control mice evaluated at the same time point (Figures 5B–5D and Table S7). Although the number of neutrophils was higher in mice evaluated at 24 h than in mice evaluated at 4 h postexposure to the flaming peat, the concentrations of TNF-α and MIP-2 were lower at 24 h, and not significantly different from saline controls. The concentration of IL-6 was also lower in mice evaluated at 24 h than in mice evaluated at 4 h postexposure, but it remained significantly higher than in saline controls. For mice exposed to the flaming peat PM, the concentrations of protein, albumin, NAG, and LDH, but not GGT, in BALF were significantly higher than saline controls evaluated at 24 h, but were not significantly different from saline controls evaluated at 4 h postexposure (Figures 5E–5I and Table S8). Thus, for most exposures, the lung toxicity potencies of the flaming PM were higher than those of the smoldering PM for neutrophils, IL-6, TNF-α, MIP-2, protein, albumin, NAG, and LDH. Mice exposed to the peat PM showed the greatest differences from controls. The statistical analysis also showed that the lung toxicity potencies were significantly associated with different fuel types and combustion phases at 24 h ($p < 0.01$) but not 4 h ($p = 0.17$) postexposure (Table S9).

Hematology analysis showed that, compared with controls, mice exposed to the smoldering eucalyptus PM had significantly lower white blood cell counts, and mice exposed to the smoldering pine PM or eucalyptus PM had significantly lower lymphocyte counts at 4 h postexposure. Mice exposed to the flaming

**Table 2.** Chemical compositions of the biomass smoke condensate collected from the multistage cryotrap system.

| | Red oak | | Peat | | Pine needles | | Pine | | Eucalyptus | |
|---|---|---|---|---|---|---|---|---|---|---|
| Component (unit) | Smoldering | Flaming | Smoldering | Flaming | Smoldering | Flaming | Smoldering | Flaming | Smoldering | Flaming |
| PM mass (mg) | 488 | 10 | 117 | 28 | 449 | 27 | 789 | 25 | 955 | 21 |
| EOM[a] (% of PM mass) | 50 | 47 | 73 | 38 | 62 | 35 | 60 | 43 | 52 | 40 |
| pH | 3.37 | 3.78 | 4.26 | 3.17 | 3.85 | 3.51 | 3.08 | 3.92 | 3.30 | 3.98 |
| Endotoxin (EU/g) | 449 | 249 | 270 | 161 | 343 | 232 | 321 | 256 | 262 | 306 |
| Ion (μg/g) | 1,285 | 155,982 | 7,148 | 339,077 | 3,379 | 143,418 | 949 | 66,625 | 330 | 65,259 |
| Ion (% of PM mass) | 0 | 16 | 1 | 34 | 0 | 14 | 0 | 7 | 0 | 7 |
| Organic carbon (μg/g) | 529,508 | 629,242 | 797,863 | 430,830 | 699,443 | 416,413 | 601,394 | 513,893 | 532,723 | 624,508 |
| Elemental carbon (μg/g) | 7,787 | 8,160 | 8,120 | 3,968 | 7,795 | 2,774 | 5,070 | 12,509 | 5,026 | 10,081 |
| Total carbon (% of PM mass) | 54 | 64 | 81 | 43 | 71 | 42 | 61 | 53 | 54 | 63 |
| Inorganic element (μg/g) | 11,081 | 91,367 | 20,559 | 131,583 | 5,505 | 56,962 | 5,920 | 42,788 | 8,045 | 51,879 |
| Inorganic element (% of PM mass) | 1 | 9 | 2 | 13 | 1 | 6 | 1 | 4 | 1 | 5 |

[a]Extractable organic matter (EOM) represents nonvolatile organic material present in the biomass smoke particulate matter (PM) that was extracted by dichloromethane.

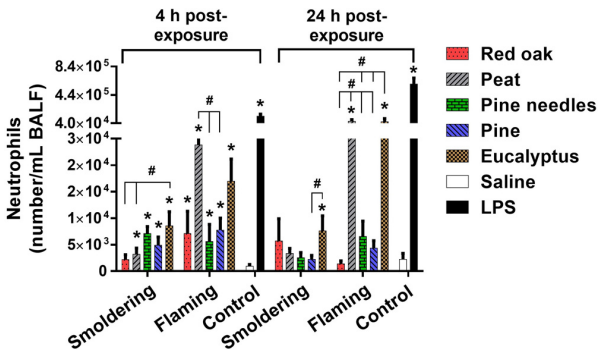


**Figure 4.** Comparative lung toxicity potencies of the biomass smoke particulate matter (PM) emitted from different fuel types and combustion phases. Lung toxicity potencies assessed from the number of neutrophils in bronchoalveolar lavage fluid (BALF) based on the equal PM mass. Mice were exposed to the PM (100 μg) by oropharyngeal aspiration, and BALF was obtained at 4 and 24 h postexposure. Data are mean ± standard error of the mean (SEM) and obtained from six mice for each group. $^{*}p < 0.05$ compared with the saline-exposed (a negative control) group from the same time point. $^{\#}p < 0.05$ compared with the different fuel group from the same combustion phase. Mice exposed to 2 μg of lipopolysaccharide (LPS) served as a positive control. The statistical tests were performed using negative binomial regression in the SAS GENMOD (version 9.4; SAS Institute Inc.) procedure.

peat, pine needles, pine, and eucalyptus PM had significantly lower white blood cell and lymphocyte counts at 4 h postexposure. At 24 h postexposure, white blood cell and lymphocyte counts were not significantly different from controls (Figure S4 and Table S10). Other hematology values (e.g., red blood cell counts, hemoglobin, and hematocrit) were not significantly different between exposed mice and controls at 4 h or 24 h postexposure.

### *Lung Toxicity Emission Factors*

In order to estimate the lung toxicity EFs, which is toxicity/mass of fuel burned, we selected only the neutrophil numbers that showed a noticeable effect in all the biomass smoke PM exposures in this study. We adjusted the neutrophil number per PM mass (referred to lung toxicity potency) for the EFs for PM (g PM/kg fuel, Table 1) and then expressed it as neutrophils/kg fuel (Figure 6 and Table S11). In contrast to the lung toxicity potencies (neutrophils/mass of PM) in which flaming conditions produced the highest values, the lung toxicity EFs (neutrophils/mass of fuel burned) of the smoldering PM were greater than those of the flaming PM at both 4 and 24 h postexposure (Figure 6 and Table S11). Under smoldering conditions, the eucalyptus PM, which had the highest EF in this study, also had the highest lung toxicity EF (i.e., the largest number of neutrophils/kg fuel) of all of the PM tested at 4 h (significantly higher than for red oak and peat) and 24 h (significantly higher for peat, pine needles, and pine), indicating that EF and the related PM exposure potencies (neutrophil counts) strongly influence the degree of lung toxicity from biomass smoke emissions. The statistical analysis showed that the lung toxicity EFs were significantly associated with different fuel types and combustion phases at 4 h ($p < 0.03$) and 24 h ($p < 0.01$) postexposure (Table S9). The lung toxicity EFs were also highly associated with emission characteristics of OC ($r^2 = 0.70$; $p < 0.01$) and PM ($r^2 = 0.74$; $p < 0.01$) in the biomass smoke (Figure S5).

### *Mutagenic Potencies of the Biomass Smoke Extractable Organic Material and Particulate Matter*

The mutagenic potencies of the EOM (rev/μg EOM) and the PM (rev/μg PM) are shown in Figures 7A and 7B and summarized in Table S12. Note that only two of the extracts (smoldering peat and pine needles in TA100 −S9) gave dose–response curves with $p$-values >0.05, which we would consider to be nonmutagenic (Figures S3G and S3H and Table S12). All the rest were mutagenic. Overall, the highest mutagenic potencies of the PM were those from flaming peat and pine, and their potencies were also significantly higher than those of the majority of other fuel PM in both strains +/−S9. Similar to the lung toxicity potencies (neutrophils/mass of PM), the mutagenic potencies of the EOM and PM (i.e., on a mass basis) were far higher under flaming phases than from smoldering phases.

The mutagenic potencies of the EOM and PM for each biomass fuel in each strain was similar with and without metabolic activation (+S9 and −S9, respectively), consistent with a mix of direct- and indirect-acting mutagenic activity. However, the EOM and PM from each biomass fuel was typically more mutagenic in TA100 than in TA98, consistent with mutagenicity due to base-substitution (vs. frameshift) mutations (Figures 7A and 7B and Table S12). All the mutagenic potencies of the PM in this study were significantly associated with different fuel types and combustion phases ($p < 0.01$) (Table S9).

### *Mutagenicity Emission Factors*

In contrast to the mutagenic potencies of the EOM and PM, for which flaming conditions were associated with the highest values (rev/mass of EOM or PM), and similar to the lung toxicity EFs, smoldering conditions were associated with the highest mutagenicity EFs (rev/mass of fuel burned) in nearly all strain/S9 combinations expressed as either rev/kg fuel or rev/$MJ_{th}$; the only exception was peat in TA100 −S9 (Figures 7C and 7D and Table S12). Pine smoke PM was associated with the highest and second-highest mutagenicity EFs (rev/kg fuel) in TA100 and TA98, respectively, under flaming conditions (statistically significant only in both strains with S9), whereas there was no statistically significant pattern of response with the smoldering PM samples. Overall, the mutagenicity EFs in TA98 + S9 were only significantly associated with different fuel types and combustion phases (Table S9). All smoldered fuels had the highest mutagenicity EFs in TA100 + S9, consistent with a dominant role of PAHs in these samples (taking into account EFs). In contrast, under flaming conditions, all PM samples had the highest mutagenicity EFs in TA100 −S9, indicating that base-substitution mutagens that were not PAHs accounted for much of these effects. The mutagenicity EFs for PM produced under flaming conditions were similar with and without S9, whereas the mutagenicity EFs of the smoldering samples were generally higher in strains supplemented with S9 than those without S9. The mutagenicity EFs were also significantly associated with emission characteristics of OC, PAHs, and PM in the biomass smoke: mutagenicity EFs in TA100 +S9 vs. EFs for OC ($r^2 = 0.90$; $p < 0.01$) and PM ($r^2 = 0.80$; $p < 0.01$); mutagenicity EFs in TA98 + S9 vs. EFs for OC ($r^2 = 0.61$; $p < 0.01$), PAHs ($r^2 = 0.53$; $p < 0.02$), and PM ($r^2 = 0.44$; $p < 0.04$); mutagenicity EFs in TA98 −S9 vs. EFs for OC ($r^2 = 0.59$; $p < 0.01$) and PM ($r^2 = 0.59$; $p < 0.01$) (Figure S6). Furthermore, the mutagenic responses in TA100 + S9 and TA98 −S9 were only associated with emission characteristics of OC and PM, and these factors were also significantly correlated with the lung toxicity EFs ($r^2 = 0.69$; $p < 0.01$ in TA100 +S9 and $r^2 = 0.42$; $p < 0.05$ in TA98 −S9) (Figure S7).

We determined mutagenicity EFs based on fuel energy used (rev/$MJ_{th}$) and compared these with the published mutagenicity EFs for various combustion emissions obtained from TA98 + S9 (Figure 8). The mutagenicity of the flaming emissions ($1.1 \times 10^5$ rev/$MJ_{th}$; average of the five fuel-burning emissions) was relatively similar

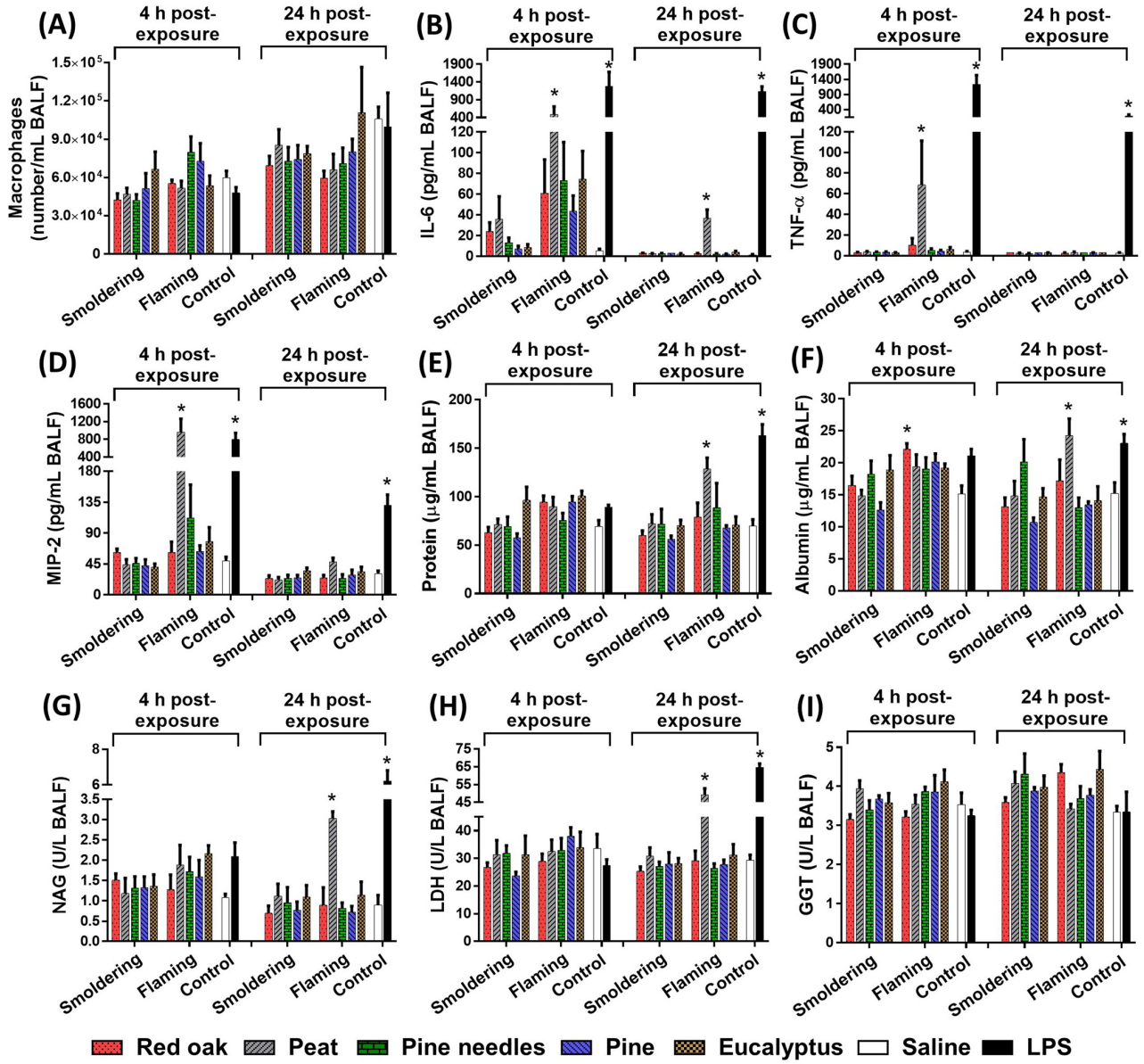


**Figure 5.** Comparative lung responses in mice exposed to the biomass smoke particulate matter (PM) emitted from different fuel types and combustion phases. (*A*) number of macrophages, concentrations of (*B*) interleukin (IL)-6, (C) tumor necrosis factor-α (TNF-α), (*D*) macrophage inhibitory protein-2 (MIP-2), (*E*) protein, (*F*) albumin, (*G*) *N*-acetyl-β-D-glucoaminidase (NAG), (*H*) lactate dehydrogenase (LDH), and (*I*) γ-glutamyl transferase (GGT) in bronchoalveolar lavage fluid (BALF) based on the equal PM mass. Mice were exposed to the PM (100 μg) by oropharyngeal aspiration, and BALF was obtained at 4 and 24 h postexposure. Data are mean ± standard error of the mean (SEM) and obtained from six mice for each group. $^*p < 0.05$ compared with the saline-exposed (a negative control) group from the same time point. Mice exposed to 2 μg of lipopolysaccharide (LPS) served as a positive control. The statistical test was performed using one-way analysis of variance (ANOVA) followed by the Dunnett's multiple comparisons.

to that of woodburning cookstove emissions ($1.3 \times 10^5$ rev/$MJ_{th}$; average of force draft stove, natural draft stove, and three-stone fire emissions; (Mutlu et al. 2016)). Although the smoldering emissions ($6.6 \times 10^5$ rev/$MJ_{th}$; average of the five fuel burning emissions) were less mutagenic than the emission from the open burning of tire [$22.7 \times 10^5$ rev/$MJ_{th}$ (DeMarini et al. 1994)], they were more mutagenic than those of diesel exhaust [$0.4 \times 10^5$ rev/$MJ_{th}$ (Mutlu et al. 2015)], municipal waste combustion [$0.4 \times 10^5$ rev/$MJ_{th}$; (Watts et al. 1992)], and the open burning of agricultural plastic [$2.5 \times 10^5$ rev/$MJ_{th}$ (Linak et al. 1989)].

## Discussion

### *Pollutant Emission Factors by Biomass Fuel Types and Combustion Phases*

Our system produced PM from well-controlled smoldering and flaming combustion that was within the respirable size range (<2.5 μm in diameter), consistent with other laboratory and field studies (McMeeking et al. 2009; Reisen et al. 2015; Ward and Hardy 1991). Moreover, the pollutant EFs for major emission constituents (CO, $CO_2$, and PM) agreed well with those from both field and laboratory measurements (Geron and Hays 2013;

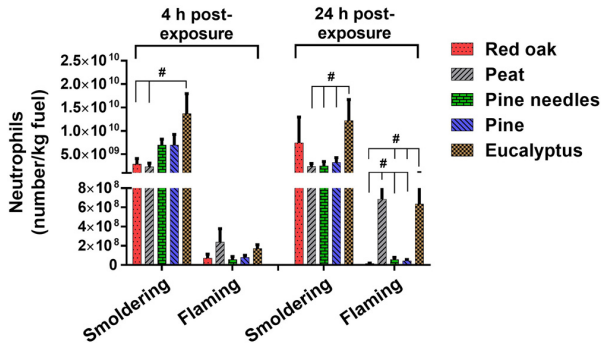


**Figure 6.** Comparative lung toxicity emission factors (EFs) of the biomass smoke particulate matter (PM) emitted from different fuel types and combustion phases. Lung toxicity emission factors (EFs) were calculated based on the emitted PM mass per mass of fuel burned. The lung toxicity potency values (neutrophils/μg PM) directly obtained from the bronchoalveolar lavage fluid (BALF) analysis (Figure 4) were converted to lung toxicity EFs (neutrophils/kg fuel) by multiplying them by the EFs for PM (g PM/kg fuel, Table 1). Data are mean ± standard error of the mean (SEM) and obtained from six mice for each group. $^{\#}p < 0.05$ compared with the different fuel group from the same combustion phase. The statistical tests were performed using negative binomial regression in the SAS GENMOD (version 9.4; SAS Institute Inc.).

McMeeking et al. 2009; Urbanski 2014). When we combined our pollutant EF data with those of others, we found high correlations between the EFs for CO, $CO_2$, and PM vs. the percent MCE. We also found that the correlations were distinguished by specific fuel types (e.g., above- and in-ground fuels). Observing this difference from uncontrolled combustions (e.g., open burning) is challenging because pollutant EFs are obtained from limited combustion phases. However, since our system produced pollutant EFs of various fuel types from a wide range of well-controlled combustion phases (60% < MCE <99%), we were able to identify strong correlations between the EFs for aboveground fuels (woods and needles) and those at in-ground level (peat or partly decayed organic matter on the forest floor called duff); note that the y-intercepts of the regression lines for the pollutant EFs as a function of MCE were quite different between the two fuel types (Figure 2). This suggests that there are distinct differences in the emission characteristics from biomass fuels from in- vs. aboveground.

In the natural environment (uncontrolled combustion), flaming and smoldering phases often occur simultaneously and are difficult to resolve (Urbanski 2014), while our system can readily distinguish between these conditions and explain the relative contributions of the different combustion phases in field measurements. For example, pollutant EFs for aboveground emissions during uncontrolled combustion were associated primarily with a flaming phase mixed with intermittent smoldering, resulting in EFs that were weighed more toward the "pure" flaming EF [see linear regression results in Figure 2; the published EFs for aboveground emissions were mostly obtained during flaming (MCE >90%)]. However, pollutant EFs from in-ground biomass combustions (peat and organic soils) were associated primarily with the pure smoldering EF [Figure 2; the published EFs for in-ground emissions were obtained mostly during smoldering (MCE >80%)]. This is consistent with a previous report (Kasischke and Bruhwiler 2002) that assumed that 80% of the emissions from aboveground biomass were produced by flaming and 20% by smoldering, whereas 80% of emissions from in-ground biomass (or 100% of peat) derived from smoldering and 20% by flaming. Overall, comparing our data to literature values suggests that pollutant EFs from controlled or uncontrolled combustion of biomass are highly dependent on the distribution of the biomass fuels vertically (aboveground or in-ground) rather than horizontally (i.e., the genus or family of wood or biomass).

### *Chemical Composition of the Biomass Smoke Condensate Relative to Fuel Types and Combustion Phases*

The cryotrap sampling system used collects and composites chemical compounds across a wide volatility range. Thus, the cryotrap samples are expected to be quite different from those collected using traditional filter-based PM and gas-phase sampling methods, which typically attempt to separate compounds by chemical and physical state. The use of the cryotrap allowed us to collect volatile and semivolatile organic compound emissions in a single sample, eliminating the well-known artifacts and interferences associated with classical sample collection (McDow and Huntzicker 1990). It also allowed us to more accurately predict specific chemical components associated with exposures to biomass smoke. OC accounted for approximately 58% of the PM mass on average. This value is similar to observations made by Kim et al. (2014b), who found that PM samples from the peat bog wildfire were comprised of 53.4% organic matter. Similarly, Reid et al. (2005) reviewed the properties of biomass-burning particles and found that the percentage of fresh smoke particles to which OC contributed varied from 13.6–67%, depending on the biomass type and combustion phase. The OC range, however, was 42–80% from nonwood (peat and pine needles) fuels, including smoldering and flaming conditions, which was wider than the 53–63% OC seen for the wood species (red oak, pine, and eucalyptus) burns (Figure 3). This variability in carbon composition is possibly explained by the fact that nonwood fuels vary more than wood fuels in their concentration of wax, cellulose, lignin, and elemental components (Hays et al. 2002).

The concentration of levoglucosan, which is a pyrolysis product of cellulose, in the smoke condensate was generally higher for the wood fuels (red oak, pine, eucalyptus) than the nonwood plant species (peat and pine needles) (Table S5). Specifically, the flaming pine and eucalyptus produced the highest levoglucosan concentrations, whereas the red oak and the two nonwood fuels showed higher concentrations during smoldering (Table S5). These findings are consistent with a larger general trend showing high levoglucosan concentrations in PM from woodburning (George et al. 2016; Hays et al. 2002; Schauer et al. 2001). Likewise, the fraction of methoxyphenols, which are lignin pyrolysis products, in the woody biomass smoke condensate was generally higher (Table S5). However, unlike levoglucosan, methoxyphenol concentrations were higher in the smoldering smoke condensate. This is consistent with the finding that methoxyphenols (wood smoke tracer compounds) are formed mainly during incomplete combustion at lower temperatures (Kjällstrand and Olsson 2004).

Previous studies show that PAH concentrations in wood smoke PM increase with combustion temperature (Bølling et al. 2012; McDonald et al. 2000; McMahon and Tsoukalas 1978; Reid et al. 2005). Presently, the PAH concentrations in the wood smoke condensate (red oak, pine, eucalyptus) were higher for flaming conditions; however, for the nonwood fuels (peat and pine needles), PAHs were higher for smoldering conditions (Table S5). Furthermore, higher combustion temperatures during flaming also increased the amount of ionic and inorganic species in the smoke condensate from flaming compared to smoldering conditions (Figure 3 and Tables S3 and S4) in agreement with a report showing that trace element concentrations for hot burning woods were two orders of magnitude higher than those for cool burning woods (Rau 1989). Similarly, Frey et al. (2009) reported that wood burning at high temperatures was associated with high emissions of ions and trace elements (20 and 1% of EF for PM,

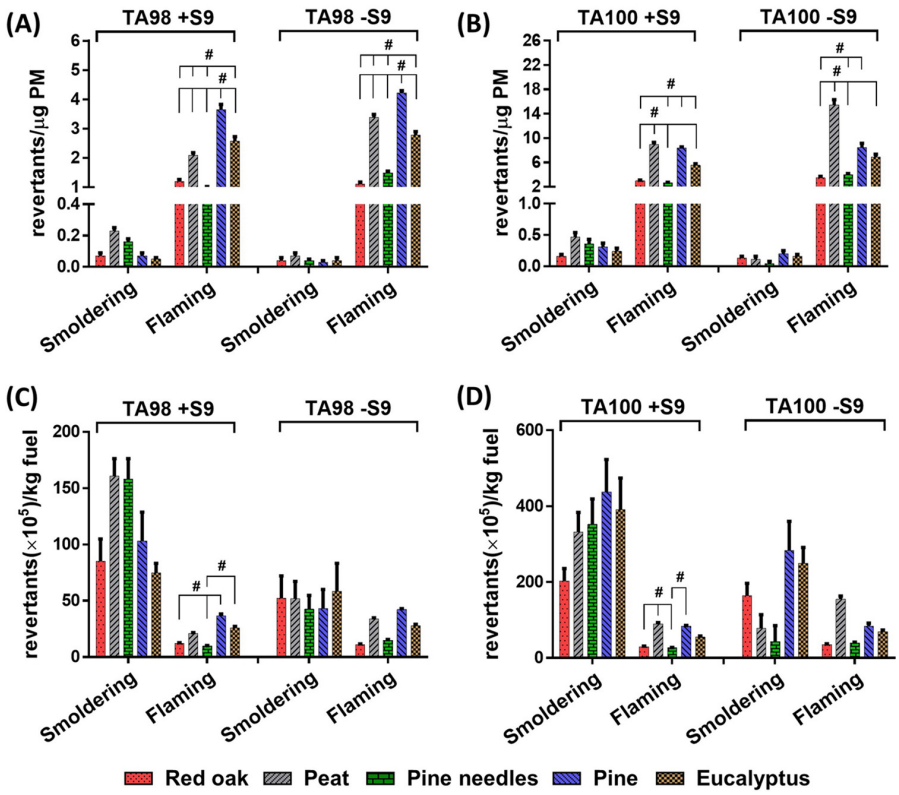


**Figure 7.** Comparative mutagenicity of the biomass smoke particulate matter (PM) emitted from different fuel types and combustion phases. (*A*) and (*B*) mutagenic potencies in strains TA98 + / − S9 and TA100 + / − S9 calculated based on the equal PM mass, and (*C*) and (*D*) mutagenicity emission factors (EFs) in strains TA98 + / − S9 and TA100 + / − S9 calculated based on the emitted PM mass per mass of fuel burned. Mutagenic potencies of the extractable organic material (EOM) were calculated from the slope of the linear portion of the dose–response curve created by the average of the primary data (rev/plate) from four independent mutagenicity experiments (Figures S2 and S3). The mutagenic potencies of the EOM were then multiplied by the percent EOM to give mutagenic potencies of the PM (rev/μg PM). These values were then converted to mutagenicity EFs (rev/kg fuel) by multiplying them by the EFs for PM (Table 1). Data are mean ± standard error of the mean (SEM) and obtained from four independent mutagenicity experiments. $^{\#}p < 0.05$ compared with the different fuel group from the same combustion phase. The statistical tests were performed using two-way factorial analysis of variance (ANOVA) in the SAS MIXED (version 9.4; SAS Institute Inc.) procedure.

respectively) compared to low temperature combustion (2 and 0.3% of EF for PM, respectively). Collectively, our findings show that the chemical composition of biomass smoke varies substantially depending on combustion conditions and fuel types, especially between wood or nonwood biomass fuels.

### *Lung Toxicity of the Biomass Smoke Particulate Matter and Role of Fuel Types and Combustion Phases*

On an equal mass basis, the flaming PM samples had higher lung toxicity (neutrophil counts) than the smoldering samples, with peat and eucalyptus being the most potent at both the 4- and 24-h time points (Figure 4). Lung injury and inflammation can be triggered by a number of different signals from both inorganic and organic moieties that cause oxidative stress in one form or another (Bølling et al. 2009; Bølling et al. 2012). The flaming peat sample had the highest levels of heavy metals (Cr, Cu, Fe, Mn, Ni, Pb, Sb, and Zn) and sulfate, many of which have been implicated in lung injury and inflammation through increased redox cycling (Fang et al. 2017; Gavett et al. 1997; Happo et al. 2013; Reiss et al. 2007; Veranth et al. 2006). On the other hand, the flaming eucalyptus had the highest levels of certain PAHs, such as phenanthrene, anthracene, and fluoranthene; the capacity for PAHs to induce oxidative stress through quinone formation is well documented (Bølling et al. 2009). The acute toxicity of eucalyptus smoke has also been linked specifically to phenolic compounds such as phenol and o-Cresol (Pimenta et al. 2000).

Although our data clearly showed stronger associations of flaming samples with toxicity markers, other studies have reported that PM from low-temperature combustion was more potent at inducing cellular damage and inflammatory cytokine release than that from high-temperature combustion (Bølling et al. 2012; Jalava et al. 2010). In some cases, the combustion conditions were less precisely controlled, and smoldering or flaming samples were taken at various periods of a complex burn that possibly reflected both combustion phases (Bølling et al. 2012). In one report, however, the results actually reflected effects based on EF and, like our study, found that flaming samples were more toxic on a mass basis; however, when adjusted for EF, the smoldering sample was more potent (Jalava et al. 2010). Thus, the smoldering PM samples from all the fuels had much higher lung toxicity when expressed as EFs, which consider both the potency of the sample as well as the amount of PM produced from a specific mass of fuel burned (Figure 6).

In addition to the combustion effect on the lung toxicity (potency and EF), the statistical analysis further demonstrated that the lung toxicity (neutrophil counts; potency and EF) from different combustion phases was also significantly associated with different fuel types (Table S9). For example, the eucalyptus or peat PM from smoldering or flaming condition had the highest lung

toxicity potency and EF at 24 h postexposure, and they were significantly higher as compared to different combustion samples (Figures 4 and 6 and Tables S6 and S11). Although the lung toxicity of the flaming eucalyptus PM was associated with high levels of PAHs, the correlation analysis showed that the lung toxicity EFs correlated better with EFs for PM and OC than with PAHs, to which it correlated poorly (Figure S5). These results indicate that the lung toxicity of the smoldering eucalyptus PM was more likely to be associated with total PM emissions than just PAHs alone. Similarly, Bølling et al. (2012) reported that the toxicity of wood smoke particles was highly associated with the organic matter, but negatively associated with the total PAH content.

### *Mutagenicity of the Biomass Smoke Particulate Matter and Role of Fuel Types and Combustion Phases*

Like the lung toxicity data, the mutagenic potencies of the PM expressed on an equal mass basis were highest for flaming samples, with pine, peat, and eucalyptus having the highest values. Of the flaming samples, the increase in the mutagenic potency of peat without S9 was higher than other fuel types, suggesting that unlike wood smoke, the organic components from peat smoke were primarily direct-acting mutagens in the *Salmonella* assay. The higher mutagenic potencies of the PM samples in TA100 vs. TA98 were consistent with findings from other studies of wood smoke (Asita et al. 1991; Mutlu et al. 2016), suggesting that the base-substitution mutagenic activity was generally more prominent than frameshift activity for these PM samples. Mutagenicity from different combustion phases was also significantly associated with different fuel types, at least for the responses expressed per unit of PM (Table S9), suggesting that the mutagenic potency of various biomass fuels in any one strain depends on the combustion phase. However, unlike the lung toxicity EF data, the mutagenicity EFs were not different between different fuel types or combustion phases except for the strain TA98 + S9 condition, suggesting that fuel types (or combustion phases) may not play a critical role in the degree of biomass smoke exposure and subsequent mutagenicity. This also supports the concept that despite having lower mutagenicity per mass, the smoldering PM produced up to 10 times more mutagenicity, resulting in an overall higher exposure and greater potential for health effects.

To understand relationships between specific chemical classes and mutagenicity EFs, we performed correlation analyses for key results. Significant correlations between mutagenicity EFs and pollutant EFs in this study were for TA100 + S9 vs. OC and TA98 + S9 vs. OC or PAHs, indicating that PAHs played an important role in the mutagenicity EFs of the fuels (Figure S6). Nitroarenes also showed positive associations with effects, as indicated by the correlation between the mutagenicity EF in TA98–S9 vs. OC or PM (Figure S6). Such results are consistent with those from other studies of biomass smoke (Asita et al. 1991; Mutlu et al. 2016). It should be pointed out, however, that like other studies (McDonald et al. 2006; Reed et al. 2006), the sum of the mass of the PAHs analyzed accounted for $<1\%$ of the mass of the PM extract (Table S5), and many other chemical classes besides PAHs and nitroarenes likely play a role in the toxicity and mutagenicity of the biomass PMs evaluated here. Interestingly, mutagenicity EFs in TA100 + S9, which detects base-substitution-inducing PAHs, correlated well with lung toxicity EFs (Figure S7), suggesting that some of the same chemical components (or components that track with these) are inducing both mutagenicity and lung toxicity. Specifically, the chemical components from the smoldering, but not the flaming, smoke emissions appeared to be responsible for both biological effects.

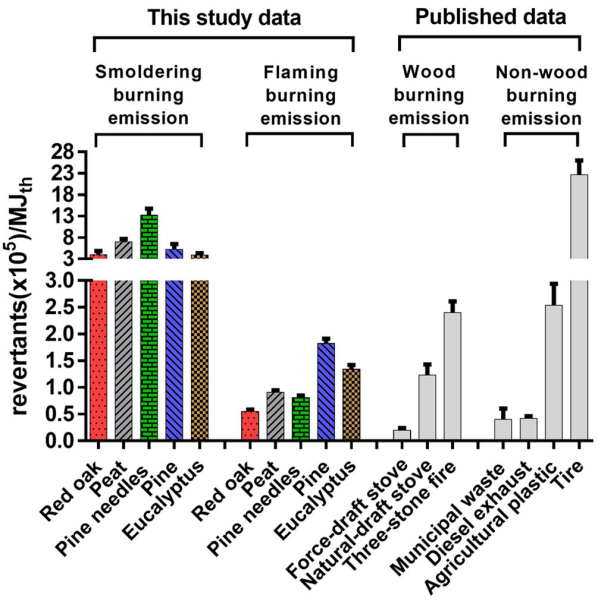


**Figure 8.** Comparison of mutagenicity emission factors (EFs) of various combustion emissions in strain TA98 + S9. The mutagenicity EFs (rev/kg fuel; Figure 7C and Table S12) were converted to rev/$MJ_{th}$ using the values for the heat energy of each fuel ($MJ_{th}$/kg fuel). The mutagenicity EFs for emissions from cookstoves burning red oak were 0.2, 1.2, and $2.4 \times 10^5$ rev/$MJ_{th}$ for the force-draft stove, natural-draft stove, and three-stone fire, respectively; data from Mutlu et al. (2016). The mutagenicity EFs for nonwood burning emissions were 0.4, 0.4, 2.5, and $22.7 \times 10^5$ rev/$MJ_{th}$ for the municipal waste, diesel exhaust, agricultural plastic, and tire, respectively; data from DeMarini et al. (1994); Linak et al. (1989); Mutlu et al. (2015); Watts et al. (1992). All data are presented as mean ± standard error of the mean (SEM).

### *Comparison of Mutagenicity Emission Factors from a Variety of Combustion Emissions*

Finally, after converting the results to megajoule$_{thermal}$($MJ_{th}$), we compared the mutagenicity EFs in TA98 + S9 to those of a variety of other combustion emissions (Figure 8), and found that the smoldering values were substantially higher than those of nearly all other combustion emissions. For example, the smoldering mutagenicity EF was found to be approximately 5, and 16 times higher than those of oak combusted in cookstoves (Mutlu et al. 2016), and of municipal waste combustion (Watts et al. 1992) or diesel exhaust (Mutlu et al. 2015), respectively. Thus, in this context, the smoldering emissions from wildland fires are highly mutagenic and support the notion that smoldering wood smoke is genotoxic and ultimately carcinogenic in humans (IARC 2010; Kato et al. 2004; Long et al. 2014).

## Conclusions

We have developed a novel combustion and smoke collection system that can be used for chemical/toxicological analyses of biomass smoke under precise combustion conditions and whose data can be used to understand the potential health effects from exposures to various biomass combustions. The lung toxicity and mutagenic potencies of biomass smoke emissions on a mass basis were greater from flaming than smoldering phases for a variety of biomass fuels; however, the EFs for these toxicological endpoints were greater for smoldering than flaming conditions. Although regulatory decisions are more relevant to the potency values (i.e., PM mass), the EFs reflect real-world exposures and should be considered in assessing the health effects of wildland fires.

Both the chemical and toxicological data illustrate the distinctive contribution of vertical vs. horizontal or wood vs. nonwood components of wildlands to the adverse biological effects of wildland fires. The greatest lung toxicity (neutrophils/kg fuel) was for eucalyptus, which is representative of chaparral-type wood, whereas the greatest mutagenicity (rev/kg fuel) was for pine, which is broadly distributed across the United States. Overall, the results suggest that emissions from fires in regions rich in those type of fuels may induce greater health effects than those from fires of similar magnitude with other types of biomass.

It should be noted that further work on *a*) more complete chemical speciation of the biomass smoke (gas and PM phase), *b*) characterization of physiologic consequences of the smoke inhalation, and *c*) disparities in health outcomes from different exposure situations (e.g., occupational, incidental, and accidental exposure) is needed to extrapolate our findings to real-world wildland fires. However, the results provide insight into the composition of forests (wood and nonwood) and the combustion conditions (smoldering and flaming) that result in emissions with decidedly distinct levels of two different types of adverse biological effects (lung toxicity and mutagenicity). Such data should provide guidance on the protection from inhalation to wildland fire smoke for firefighter and public health responses to wildland fires, whose scale and severity are increasing worldwide.

## Acknowledgments

The authors would like to thank C. Copeland, L. Copeland, W. Williams, D. Andrews, and J. Richards for technical assistance in toxicological analyses; J. McGee and K. Kovalcik for technical assistance in PM chemical analyses; S. Urbanski (Missoula Fire Sciences Laboratory) for kindly providing biomass samples; and S. Gavett and W. P. Linak for their careful review of this manuscript.

This study was supported by the Joint Fire Science Program Project (14-1-04-16) and was performed while Y.H.K. held a National Research Council Senior Research Associateship Award at the U.S. EPA. Additional support was provided by the intramural research program of the Office of Research and Development, U.S. EPA, Research Triangle Park, North Carolina.

The research described in this manuscript has been reviewed by the National Health and Environmental Effects Research Laboratory, U.S. EPA, and approved for publication. Approval does not signify that contents necessarily reflect the views and policies of the agency, nor does the mention of trade names or commercial products constitute endorsement or recommendation for use.

## References

Abatzoglou JT, Williams AP. 2016. Impact of anthropogenic climate change on wildfire across western US forests. Proc Natl Acad Sci U S A 113(42):11770–11775, PMID: 27791053, https://doi.org/10.1073/pnas.1607171113.

Adetona O, Reinhardt TE, Domitrovich J, Broyles G, Adetona AM, Kleinman MT, et al. 2016. Review of the health effects of wildland fire smoke on wildland firefighters and the public. Inhal Toxicol 28(3):95–139, PMID: 26915822, https://doi.org/10.3109/08958378.2016.1145771.

Asita AO, Matsui M, Nohmi T, Matsuoka A, Hayashi M, Ishidate M, Jr., et al. 1991. Mutagenicity of wood smoke condensates in the *Salmonella*/microsome assay. Mutat Res 264(1):7–14, PMID: 1881415, https://doi.org/10.1016/0165-7992(91)90039-7.

Bell DA, Kamens RM. 1990. Evaluation of the mutagenicity of combustion particles from several common biomass fuels in the Ames/*Salmonella* microsome test. Mutat Res 245(3):177–183, PMID: 2233838, https://doi.org/10.1016/0165-7992(90)90047-N.

Bide RW, Armour SJ, Yee E. 2000. Allometric respiration/body mass data for animals to be used for estimates of inhalation toxicity to young adult humans. J Appl Toxicol 20(4):273–290, PMID: 10942903, https://doi.org/10.1002/1099-1263(200007/08)20:4%3C273::AID-JAT657%3E3.0.CO;2-X.

Bølling AK, Pagels J, Yttri KE, Barregard L, Sallsten G, Schwarze PE, et al. 2009. Health effects of residential wood smoke particles: the importance of combustion conditions and physicochemical particle properties. Part Fibre Toxicol 6:29, PMID: 19891791, https://doi.org/10.1186/1743-8977-6-29.

Bølling AK, Totlandsdal AI, Sallsten G, Braun A, Westerholm R, Bergvall C, et al. 2012. Wood smoke particles from different combustion phases induce similar pro-inflammatory effects in a co-culture of monocyte and pneumocyte cell lines. Part Fibre Toxicol 9:45, PMID: 23176191, https://doi.org/10.1186/1743-8977-9-45.

Burling IR, Yokelson RJ, Griffith DWT, Johnson TJ, Veres P, Roberts JM, et al. 2010. Laboratory measurements of trace gas emissions from biomass burning of fuel types from the southeastern and southwestern United States. Atmos Chem Phys 10(22):11115–11130, https://doi.org/10.5194/acp-10-11115-2010.

de Muñiz GIB, Lengowski EC, Nisgoski S, de Magalhães WLE, de Oliveira VT, Hansel F. 2014. Characterization of *Pinus* spp needles and evaluation of their potential use for energy. Cerne 20(2):248–250, https://doi.org/10.1590/01047760.201420021358.

De Vleeschouwer F, Chambers FM, Swindles GT. 2010. Coring and sub-sampling of peatlands for palaeoenvironmental research. Mires Peat 7:1–10.

DeMarini DM, Lemieux PM, Ryan JV, Brooks LR, Williams RW. 1994. Mutagenicity and chemical analysis of emissions from the open burning of scrap rubber tires. Environ Sci Technol 28(1):136–141, PMID: 22175842, https://doi.org/10.1021/es00050a018.

Diggle PJ, Heagerty PJ, Liang KY, Zeger SL. 2002. *Analysis of Longitudinal Data*. 2nd edition. New York, NY:Oxford University Press.

Fang T, Guo H, Zeng L, Verma V, Nenes A, Weber RJ. 2017. Highly acidic ambient particles, soluble metals, and oxidative potential: a link between sulfate and aerosol toxicity. Environ Sci Technol 51(5):2611–2620, PMID: 28141928, https://doi.org/10.1021/acs.est.6b06151.

Frey AK, Tissari J, Saarnio KM, Timonen HJ, Tolonen-Kivimäki O, Aurela MA, et al. 2009. Chemical composition and mass size distribution of fine particulate matter emitted by a small masonry heater. Boreal Env Res 14:255–271.

Fröhlich E, Mercuri A, Wu S, Salar-Behzadi S. 2016. Measurements of deposition, lung surface area and lung fluid for simulation of inhaled compounds. Front Pharmacol 7:181, PMID: 27445817, https://doi.org/10.3389/fphar.2016.00181.

Gavett SH, Madison SL, Dreher KL, Winsett DW, McGee JK, Costa DL. 1997. Metal and sulfate composition of residual oil fly ash determines airway hyperreactivity and lung injury in rats. Environ Res 72(2):162–172, PMID: 9177658, https://doi.org/10.1006/enrs.1997.3732.

George IJ, Black RR, Geron CD, Aurell J, Hays MD, Preston WT, et al. 2016. Volatile and semivolatile organic compounds in laboratory peat fire emissions. Atmos Environ 132:163–170, https://doi.org/10.1016/j.atmosenv.2016.02.025.

Geron C, Hays M. 2013. Air emissions from organic soil burning on the coastal plain of North Carolina. Atmos Environ 64:192–199, https://doi.org/10.1016/j.atmosenv.2012.09.065.

Gilman JB, Lerner BM, Kuster WC, Goldan PD, Warneke C, Veres PR, et al. 2015. Biomass burning emissions and potential air quality impacts of volatile organic compounds and other trace gases from fuels common in the US. Atmos Chem Phys 15(24):13915–13938, https://doi.org/10.5194/acp-15-13915-2015.

Gilmour MI, McGee J, Duvall RM, Dailey L, Daniels M, Boykin E, et al. 2007. Comparative toxicity of size-fractionated airborne particulate matter obtained from different cities in the United States. Inhal Toxicol 19 (suppl 1):7–16, PMID: 17886044, https://doi.org/10.1080/08958370701490379.

Happo MS, Uski O, Jalava PI, Kelz J, Brunner T, Hakulinen P, et al. 2013. Pulmonary inflammation and tissue damage in the mouse lung after exposure to PM samples from biomass heating appliances of old and modern technologies. Sci Total Environ 443:256–266, PMID: 23201646, https://doi.org/10.1016/j.scitotenv.2012.11.004.

Hays MD, Geron CD, Linna KJ, Smith ND, Schauer JJ. 2002. Speciation of gas-phase and fine particle emissions from burning of foliar fuels. Environ Sci Technol 36(11):2281–2295, PMID: 12075778, https://doi.org/10.1021/es0111683.

IARC (International Agency for Research on Cancer). 2010. Household use of solid fuels and high-temperature frying. *IARC Monographs on the evaluation of Carcinogenic Risks to Humans*, Vol. 95. Lyon, France:International Agency for Research on Cancer (IARC) Working Group.

Ince PJ. 1979. How to Estimate Recoverable Heat Energy in Wood or Bark Fuels. Madison, Wisconsin:U.S. Department of Agriculture, Forest Service, Forest Products Laboratory.

Jalava PI, Salonen RO, Nuutinen K, Pennanen AS, Happo MS, Tissari J, et al. 2010. Effect of combustion condition on cytotoxic and inflammatory activity of residential wood combustion particles. Atmos Environ 44(13):1691–1698, https://doi.org/10.1016/j.atmosenv.2009.12.034.

Johnston FH, Henderson SB, Chen Y, Randerson JT, Marlier M, Defries RS, et al. 2012. Estimated global mortality attributable to smoke from landscape fires. Environ Health Perspect 120(5):695–701, PMID: 22456494, https://doi.org/10.1289/ehp.1104422.

Kasischke ES, Bruhwiler LP. 2002. Emissions of carbon dioxide, carbon monoxide, and methane from boreal forest fires in 1998. J Geophys Res-Atmos 107:FFR 2-1–FFR 2-14, https://doi.org/10.1029/2001JD000461.

Kato M, Loomis D, Brooks LM, Gattas GF, Gomes L, Carvalho AB, et al. 2004. Urinary biomarkers in charcoal workers exposed to wood smoke in Bahia State, Brazil. Cancer Epidemiol Biomarkers Prev 13(6):1005–1012, PMID: 15184257.

Kellison RC, Lea R, Marsh P. 2013. Introduction of *Eucalyptus* spp. into the United States with special emphasis on the southern United States. Int J Forest Res 2013:9, https://doi.org/10.1155/2013/189393.
Kim YH, Boykin E, Stevens T, Lavrich K, Gilmour MI. 2014a. Comparative lung toxicity of engineered nanomaterials utilizing in vitro, *ex vivo* and *in vivo* approaches. J Nanobiotechnology 12:47, PMID: 25424549, https://doi.org/10.1186/s12951-014-0047-3.
Kim YH, Tong H, Daniels M, Boykin E, Krantz QT, McGee J, et al. 2014b. Cardiopulmonary toxicity of peat wildfire particulate matter and the predictive utility of precision cut lung slices. Part Fibre Toxicol 11:29, PMID: 24934158, https://doi.org/10.1186/1743-8977-11-29.
Kim YH, Wyrzykowska-Ceradini B, Touati A, Krantz QT, Dye JA, Linak WP, et al. 2015. Characterization of size-fractionated airborne particles inside an electronic waste recycling facility and acute toxicity testing in mice. Environ Sci Technol 49(19):11543–11550, PMID: 26332991, https://doi.org/10.1021/acs.est.5b03263.
Kjällstrand J, Olsson M. 2004. Chimney emissions from small-scale burning of pellets and fuelwood—examples referring to different combustion appliances. Biomass Bioenergy 27(6):557–561, https://doi.org/10.1016/j.biombioe.2003.08.014.
Klimisch H-J, Hollander HWM, Thyssen J. 1980. Generation of constant concentrations of thermal decomposition products in inhalation chambers. A comparative study with a method according to din 53436. I. Measurement of carbon monoxide and carbon dioxide in inhalation chambers. J Combust Toxicol 7:243–256.
Landis MS, Edgerton ES, White EM, Wentworth GR, Sullivan AP, Dillner AM. 2017. The impact of the 2016 Fort Mcmurray Horse River Wildfire on ambient air pollution levels in the Athabasca Oil Sands Region, Alberta, Canada. Sci Total Environ (17):32695–32695, PMID: 29102183, https://doi.org/10.1016/j.scitotenv.2017.10.008.
Lawless JF. 1987. Negative binomial and mixed poisson regression. Can J Statistics 15(3):209–225, https://doi.org/10.2307/3314912.
Levine JS, Bobbe T, Ray N, Witt R, Singh A. 1999. Wildland Fires and the Environment: A Global Synthesis. UNEP/DEIAEW/TR99-1. http://citeseerx.ist.psu.edu/viewdoc/download?doi=10.1.1.566.8641&rep=rep1&type=pdf [accessed 29 December 2017].
Linak WP, Ryan JV, Perry E, Williams RW, DeMarini DM. 1989. Chemical and biological characterization of products of incomplete combustion from the simulated field burning of agricultural plastic. JAPCA 39(6):836–846, PMID: 2754442, https://doi.org/10.1080/08940630.1989.10466570.
Liu JC, Pereira G, Uhl SA, Bravo MA, Bell ML. 2015. A systematic review of the physical health impacts from non-occupational exposure to wildfire smoke. Environ Res 136:120–132, PMID: 25460628, https://doi.org/10.1016/j.envres.2014.10.015.
Long AS, Lemieux CL, Yousefi P, Ruiz-Mercado I, Lam NL, Orellana CR, et al. 2014. Human urinary mutagenicity after wood smoke exposure during traditional temazcal use. Mutagenesis 29(5):367–377, PMID: 25084778, https://doi.org/10.1093/mutage/geu025.
Maron DM, Ames BN. 1983. Revised methods for the *Salmonella* mutagenicity test. Mutat Res 113(3-4):173–215, PMID: 6341825, https://doi.org/10.1016/0165-1161(83)90010-9.
McDonald JD, White RK, Barr EB, Zielinska B, Chow JC, Grosjean E. 2006. Generation and characterization of hardwood smoke inhalation exposure atmospheres. Aerosol Sci Technol 40(8):573–584, https://doi.org/10.1080/02786820600724378.
McDonald JD, Zielinska B, Fujita EM, Sagebiel JC, Chow JC, Watson JG. 2000. Fine particle and gaseous emission rates from residential wood combustion. Environ Sci Technol 34(11):2080–2091, https://doi.org/10.1021/es9909632.
McDow SR, Huntzicker JJ. 1990. Vapor adsorption artifact in the sampling of organic aerosol: face velocity effects. Atmos Environ Part A 24(10):2563–2571, https://doi.org/10.1016/0960-1686(90)90134-9.
McMahon CK, Tsoukalas SN. 1978. Polynuclear aromatic hydrocarbons in forest fire smoke. *Carcinogenesis, Vol. 3: Polynuclear Aromatic Hydrocarbons*. Jones PW, Freudenthal RI, eds. New York, NY:Raven Press, 61–73.
McMeeking GR, Kreidenweis SM, Baker S, Carrico CM, Chow JC, Collett JL, et al. 2009. Emissions of trace gases and aerosols during the open combustion of biomass in the laboratory. J Geophys Res 114(D19):D19210, https://doi.org/10.1029/2009JD011836.
Morvay ZK, Gvozdenac DD. 2008. Part III: Toolbox. *Fundamentals for Analysis and Calculation of Energy and Environmental Performance*. West Sussex, UK:John Wiley & Sons.
Mutlu E, Warren SH, Ebersviller SM, Kooter IM, Schmid JE, Dye JA, et al. 2016. Mutagenicity and pollutant emission factors of solid-fuel cookstoves: comparison with other combustion sources. Environ Health Perspect 124(7):974–982, PMID: 26895221, https://doi.org/10.1289/ehp.1509852.
Mutlu E, Warren SH, Matthews PP, Schmid JE, Kooter IM, Linak WP, et al. 2015. Health effects of soy-biodiesel emissions: bioassay-directed fractionation for mutagenicity. Inhal Toxicol 27(11):597–612, PMID: 26514787, https://doi.org/10.3109/08958378.2015.1091054.
Naeher LP, Brauer M, Lipsett M, Zelikoff JT, Simpson CD, Koenig JQ, et al. 2007. Woodsmoke health effects: a review. Inhal Toxicol 19(1):67–106, PMID: 17127644, https://doi.org/10.1080/08958370600985875.
Nielson RW, Dobie J, Wright DM. 1985. *Conversion Factors for the Forest Product Industry in Western Canada*. Vancouver, BC, Canada:Forintek Canada Corp Western Laboratory.
NRC (National Research Council). 1992. *Guideline for Developing Spacecraft Maximum Allowable Concentrations for Space Station Contaminants*. Washington, DC:National Academy Press.
Pimenta AS, Bayona JM, García MT, Solanas AM. 2000. Evaluation of acute toxicity and genotoxicity of liquid products from pyrolysis of *Eucalyptus grandis* wood. Arch Environ Contam Toxicol 38(2):169–175, PMID: 10629278, https://doi.org/10.1007/s002449910022.
Porwollik S, Wong RM, Sims SH, Schaaper RM, DeMarini DM, McClelland M. 2001. The ΔuvrB mutations in the Ames strains of *Salmonella* span 15 to 119 genes. Mutat Res 483(1–2):1–11, PMID: 11600126, https://doi.org/10.1016/S0027-5107(01)00239-1.
Rau JA. 1989. Composition and size distribution of residential wood smoke particles. Aerosol Sci Technol 10(1):181–192, https://doi.org/10.1080/02786828908959233.
Reed MD, Campen MJ, Gigliotti AP, Harrod KS, McDonald JD, Seagrave JC, et al. 2006. Health effects of subchronic exposure to environmental levels of hardwood smoke. Inhal Toxicol 18(8):523–539, PMID: 16717024, https://doi.org/10.1080/08958370600685707.
Reid CE, Brauer M, Johnston FH, Jerrett M, Balmes JR, Elliott CT. 2016. Critical review of health impacts of wildfire smoke exposure. Environ Health Perspect 124(9):1334–1343, PMID: 27082891, https://doi.org/10.1289/ehp.1409277.
Reid JS, Koppmann R, Eck TF, Eleuterio DP. 2005. A review of biomass burning emissions part II: intensive physical properties of biomass burning particles. Atmos Chem Phys 5(3):799–825, https://doi.org/10.5194/acp-5-799-2005.
Reisen F, Duran SM, Flannigan M, Elliott C, Rideout K. 2015. Wildfire smoke and public health risk. Int J Wildland Fire 24(8):1029–1044, https://doi.org/10.1071/WF15034.
Reiss R, Anderson EL, Cross CE, Hidy G, Hoel D, McClellan R, et al. 2007. Evidence of health impacts of sulfate-and nitrate-containing particles in ambient air. Inhal Toxicol 19(5):419–449, PMID: 17365047, https://doi.org/10.1080/08958370601174941.
Schauer JJ, Kleeman MJ, Cass GR, Simoneit BR. 2001. Measurement of emissions from air pollution sources. 3. $C_1$–$C_{29}$ organic compounds from fireplace combustion of wood. Environ Sci Technol 35(9):1716–1728, PMID: 11355184, https://doi.org/10.1021/es001331e.
Schmid O, Stoeger T. 2016. Surface area is the biologically most effective dose metric for acute nanoparticle toxicity in the lung. J Aerosol Sci 99:133–143, https://doi.org/10.1016/j.jaerosci.2015.12.006.
Soares Neto TG, Carvalho JA, Jr, Veras CAG, Alvarado EC, Gielow R, Lincoln EN, et al. 2009. Biomass consumption and $CO_2$, CO and main hydrocarbon gas emissions in an Amazonian forest clearing fire. Atmos Environ 43(2):438–446, https://doi.org/10.1016/j.atmosenv.2008.07.063.
Straif K, Baan R, Grosse Y, Secretan B, El Ghissassi F, Cogliano V. 2006. Carcinogenicity of household solid fuel combustion and of high-temperature frying. Lancet Oncol 7(12):977–978, PMID: 17348122, https://doi.org/10.1016/S1470-2045(06)70969-X.
Swiston JR, Davidson W, Attridge S, Li GT, Brauer M, van Eeden SF. 2008. Wood smoke exposure induces a pulmonary and systemic inflammatory response in firefighters. Eur Respir J 32(1):129–138, PMID: 18256060, https://doi.org/10.1183/09031936.00097707.
Urbanski S. 2014. Wildland fire emissions, carbon, and climate: emission factors. Forest Ecol Manage 317:51–60, https://doi.org/10.1016/j.foreco.2013.05.045.
Veranth JM, Moss TA, Chow JC, Labban R, Nichols WK, Walton JC, et al. 2006. Correlation of in vitro cytokine responses with the chemical composition of soil-derived particulate matter. Environ Health Perspect 114(3):341–349, PMID: 16507455, https://doi.org/10.1289/ehp.8360.
Ward DE, Hardy CC. 1991. Smoke emissions from wildland fires. Environ Int 17(2–3):117–134, https://doi.org/10.1016/0160-4120(91)90095-8.
Ward DE, Radke LF. 1993. Emissions measurements from vegetation fires: A comparative evaluation of methods and results. *Fire in the Environment: The Ecological, Atmospheric, and Climatic Importance of Vegetation Fires*. Crutzen PJ, Goldammer JG, eds. Chichester, UK:John Wiley & Sons.
Watts RR, Lemieux PM, Grote RA, Lowans RW, Williams RW, Brooks LR, et al. 1992. Development of source testing, analytical, and mutagenicity bioassay procedures for evaluating emissions from municipal and hospital waste combustors. Environ Health Perspect 98:227–234, PMID: 1486854, https://doi.org/10.1289/ehp.9298227.
Weibel ER. 1973. Morphological basis of alveolar-capillary gas exchange. Physiol Rev 53(2):419–495, PMID: 4581654, https://doi.org/10.1152/physrev.1973.53.2.419.
Werley MS, Lee KM, Lemus-Olalde R. 2009. Toxicological responses in SW mice exposed to inhaled pyrolysates of polymer/tobacco mixtures and blended tobacco. Inhal Toxicol 21(14):1186–1199, PMID: 19922405, https://doi.org/10.3109/08958370902803073.
Westerling AL, Hidalgo HG, Cayan DR, Swetnam TW. 2006. Warming and earlier spring increase western U.S. Forest wildfire activity. Science 313(5789):940–943, PMID: 16825536, https://doi.org/10.1126/science.1128834.